

MUON PHYSICS*

W. T. Toner

Stanford Linear Accelerator Center
Stanford University, Stanford, California 94305

(Invited Paper Presented at the 1969 International Conference on
Electron and Photon Interactions at High Energies, Daresbury,
England, September 1969)

* Work supported by the U. S. Atomic Energy Commission.

I. INTRODUCTION

In this talk, I will discuss experiments with high energy muons which have recently been completed or are in progress. Brodsky¹ has discussed quantum electrodynamical aspects of muon physics, and weak interactions are appropriate to other meetings. The main problem in muon physics is, of course, that we do not understand why it should exist. As far as the muon is concerned, it seems only to have the purpose of mystifying us. Indeed, the only dramatic thing that I know would happen if the muon did not exist is that the pion would live 10^4 times as long as it does now. And I am unable to think of any very obvious consequences of that change.

High energy muon scattering should be completely dominated by the electromagnetic interaction, and the electromagnetic interactions of the muon are very well understood; indeed, the muon g-2 experiment² testifies to the ability of the theorists to calculate,³ as well as to the ability of the experimentalists to measure. The calculations involve integrations which include the effects of interactions at very high momentum transfer, and it is hard to see how any phenomenon that would produce an obvious effect in muon scattering would not also produce an effect in g-2 which would be measurable, granted the precision with which these experiments are done. Farley⁴ and Bailey and Picasso⁵ have given detailed discussions of the sensitivity of the g-2 experiment to a variety of possible high momentum transfer anomalies. In particular, if the muon is given a form factor of the type $\left(1 + \frac{q^2}{\Lambda^2}\right)^{-1}$, the most recent results establish $\Lambda_\mu > 7$ GeV, with 95% confidence. However, the comparison of muon scattering with electron scattering tests the equality of the muon and electron vertex in a very direct way. The

results of a comparison of muon scattering with electron scattering, combined with limits on the muon vertex obtained from the g-2 experiment can set limits on the electron vertex.¹ Experimentalists maintain a stubborn conviction that if only violent enough collisions are induced, something obvious will happen. This may be somewhat naive, but since similar considerations provide much of the force driving high energy physics as a whole towards the construction of bigger and better accelerators, I do not see why I should have to argue further on this score. We can be sure that the solution to the μ -e problem will be as unexpected as it is puzzling.

Finally, there is always the possibility that muons may be a better tool than electrons for exploring some aspects of particle physics, on account of the smaller electromagnetic backgrounds and corrections resulting from the larger mass of the muon. The time may not be far off when this possibility becomes a reality.

II. MUON TRIDENTS

A muon trident results when a muon interacts in the Coulomb field of a nucleus to produce a muon pair. This is the only reaction so far observed which has two muons of the same sign in the final state, and which therefore gives us an opportunity to see if muons are subject to the exclusion principle. In a paper presented to this conference, J. J. Russel et al.,⁶ report on the analysis of 89 tridents produced by 11 GeV muons on Pb. It is the first conclusive demonstration that the process takes place. The experimental arrangement is shown in Fig. 1. The angles and momenta of the incident muon and of all three final state muons were measured in optical spark chambers. The trigger required two or more final state muons, one with charge opposite to that of the beam muons. Runs were made with positive and

negative muons incident. The analysis has been performed in terms of the invariant mass of the pair of like muons, M_{like} . For $M_{\text{like}} = 2\mu$, where μ is the mass of the muon, the cross section is depressed by the Pauli principle. The experiment is more sensitive than one might expect from the small number of total events observed and the number of kinematic variables. This is due to the cross section being very strongly biased towards small values of the pair invariant mass, so that most of the events are close to where the exclusion effect would be seen. Two exactly identical muons would be rather difficult to detect: an experimental exclusion effect operates. Fortunately, the uncertainty principle produces a smearing which spreads the depression in the cross section out over a region of invariant mass of the order of the muon mass above minimum. For muons emerging with the same momentum p , with an opening angle θ , the invariant mass of the pair is $2\mu \left[1 + \left(\frac{p \sin \theta/2}{\mu} \right)^2 \right]^{1/2}$. Therefore, the opening angles must be quite small for the effect to be seen. However, the energies of the two like muons can be substantially different without much change in the invariant mass. The invariant mass of a pair with energies E_1, E_2 but with no opening angle is $2\mu \left(1 + \frac{(E_1 - E_2)^2}{4E_1 E_2} \right)^{1/2}$. The momentum analysis of all three final state muons spreads the like muons apart quite effectively. Therefore, detection efficiency effects are expected to depend only on the pair opening angle. To check for the absence of such bias, the analysis was repeated for the unlike pairs and no loss of events at small pair mass was seen.

The invariant mass distribution of the like pairs is shown in Fig. 2a. A 2-1/2 standard deviation suppression below the "no-exchange graph" predictions is observed in the lowest bin, and the results are in very satisfactory agreement with what is expected for fermions. The agreement with theory of the two possible unlike combinations, shown in Fig. 2b and Fig. 2c is unfortunately less

spectacular. The total number of pairs found, 89 ± 9 , is in satisfactory agreement with the value predicted for fermions of 82 ± 2 . It does not agree with the value of 112 ± 2 which would be obtained if the exchange graphs were ignored. The muon would appear to be a fermion, although the experiment has insufficient statistics to establish the result as firmly as one would like.

III. ELASTIC MUON SCATTERING

The elastic scattering cross section is given by the familiar Rosenbluth formula:⁷

$$\frac{d\sigma}{dq^2} = \frac{d\sigma}{dq_{ns}^2} \operatorname{tg}^2 \frac{\theta}{2} \left[\frac{q^2}{2M^2} G_M^2(q^2) + \frac{\left(G_E^2 + \frac{q^2}{4M^2} G_M^2 \right)}{1 + \frac{q^2}{4M^2}} \cot^2 \frac{\theta}{2} \right] \quad (1)$$

where $\frac{d\sigma}{dq_{ns}^2}$ is the result for a spinless point proton, θ is the laboratory scattering angle of the muon, q^2 the square of the four-momentum transfer (here positive for space-like values) and M is the nucleon mass. G_E and G_M are the nucleon form factors measured in electron scattering. The mass of the muon is unimportant at high energies. Detailed formulae incorporating lepton masses and form factors due to Barnes⁸ are discussed in the review of Lederman and Tannenbaum.⁹ On dividing the observed cross section by the first two terms on the right-hand side of Eq. (1), we get the term in brackets, which should show the well established straight-line dependence¹⁰ when plotted at constant q^2 as a function of $\cot^2 \frac{\theta}{2}$. The low q^2 limit of Eq. (1) is given by the static properties of the particles; any μ -e difference would be extremely unlikely in this limit.

Previous experiments on μ -p elastic scattering have given results in agreement with electron scattering, apart from a normalization discrepancy in the experiment of Ellsworth et al.¹¹ However, the authors did not consider that the discrepancy

established a muon-electron difference, although they could not find any good experimental reason for it. This summer, results from the new Columbia-Rochester experiment have been published.¹² Negative muons of 6, 11 and 17 GeV/c and positive muons of 6 and 11 GeV/c momentum were used. The beam had a 15% momentum resolution and a 7.5 cm by 15 cm cross sectional area. The experiment is shown in Fig. 3. The muons scattered in a 1.2 m liquid hydrogen target. The angles of the incident and scattered muons and of the recoil proton were measured in thin plate spark chambers. Trigger requirements were that the muon should scatter through more than 15 mrad (defined by hodoscope counter arrays in the incident and scattered beam), that there be a proton recoil and that there be no veto. In addition, the muons were required to penetrate 1.8 m of uranium. Reconstruction precision was good, coplanarity was measured to 1.7 mrad, and the vertex was defined to 0.5 cm. The kinematics can be determined entirely from the angles, given the assumption of elastic scattering. The range of the recoil proton observed in range chambers was used as a check on the reconstruction. The distribution of the differences between the ranges calculated from the angles and those measured was in agreement with a Monte-Carlo simulation of the experiment. In particular, there was no shift of the peak position. This is important, since it confirms that the value of q^2 is well determined. It was not required that the recoil have the correct range in order for the event to be acceptable. In the experiment of Ellsworth et al.,¹¹ the momentum transfer was determined by range and significant corrections at high-momentum transfer were needed to include the effects on the cross section of the interactions of the recoil. In the present experiment it was found that the coplanarity requirement plus a very loose cut on the calculated momentum of the incident muon was sufficient to give a clean sample of events. The subtraction of noncoplanar events was 2%. The authors are very

confident that they understand the details of the beam and apparatus, since their Monte-Carlo simulation of the experiment agrees very well with observations at all verifiable points.

The apparatus did not contain a magnet, and the properties of the positive and negative muon beams were found to be identical, so that their first result is completely independent of any possible systematic bias. A comparison of μ^+ and μ^- cross sections gave a mean value of

$$\frac{\sigma(\mu^+) - \sigma(\mu^-)}{\sigma(\mu^+) + \sigma(\mu^-)} = 0.015 \pm 0.012$$

A fit with no asymmetry gave a χ^2 of 10.5 for 13 degrees of freedom. A sample of their data exhibiting the Rosenbluth straight line is shown in Fig. 4. They found it possible to neglect $\frac{q^2}{2M^2} G_M^2$ in comparison with the term multiplied by $\cot^2 \frac{\theta}{2}$ in Eq. (1). With that simplification they could easily combine all their data, and arrived at a χ^2 of 17.8 for 24 degrees of freedom for the straight line hypothesis. They make the point that their measurements extend to $\cot^2 \frac{\theta}{2}$ values far in excess of electron data published to date. Departures from linearity and from μ^+/μ^- symmetry would be caused by two-photon exchange. They conclude that the contribution of two-photon exchange amplitude in both 2^+ and $1^+ J^P$ states is less than 4%.

The results for the values of the form factors are shown in Fig. 5. The muon data and the data of Janssens et al.¹³ have each been analyzed¹² to extract the slope of the straight line under the scaling law assumption $G_E = G_M/\mu = G$. It is immediately obvious from Fig. 5 that there is a discrepancy which looks like a normalization error. They have made an analysis which assumes $\frac{G_\mu}{G_e} = \frac{N}{1+q^2/\Lambda^2}$. A value of $N = 1.0$ would imply perfect normalization. If $N = 1.0$ is used, the fit to the data gives $1/\Lambda^2 = .148 \pm .024$, very significantly different from zero. If $1/\Lambda^2 = 0$

is used, then $N = 0.96$. Since the square of the form factor enters into the cross section, the normalization error in the cross section would be 8%. The authors find it difficult to account for an error of this magnitude, but have not published an estimate of what they would expect their "standard deviation" normalization uncertainty to be, so that it is difficult to judge the statistical significance of the results. They note that the Ellsworth data (which has a 16% discrepancy in the normalization of the cross section when analyzed in this fashion) is in agreement with their present data. As a final result they quote values for N and $1/\Lambda^2$ obtained from a fit which allowed both to be free parameters, giving $N = .976 \pm .017$ and $1/\Lambda^2 = .064 \pm .056 \text{ (GeV/c)}^{-2}$. The statistical errors are in the fit. They claim, with 95% confidence, that $\Lambda > 2.4 \text{ GeV/c}$.

The main statistical weight of the muon data is centered around a $|q^2|$ of $.28 \text{ (GeV/c)}^2$: the values of N and $1/\Lambda^2$ quoted above all lead to a $\frac{G_\mu}{G_e}$ ratio of $.96$ at this value of $|q^2|$. The new data of the Bonn group reported to this conference¹⁴ seem to lie a little below Janssen's data used in the μ -e comparison in this q^2 range, and appear to be lowest at the smallest values of q^2 . It would be interesting to see a comparison of the muon scattering results with these new data.

The systematic uncertainties of the electron scattering experiments taken individually seem to be similar to those of the muon experiment. The techniques used in the muon scattering experiments are still capable of improvement, whereas the electron scattering techniques may already have reached a degree of sophistication which makes substantial improvements in systematic uncertainties unlikely, or at least extremely difficult. It may well be that muon scattering would be the best means of determining the form factors in the range $0.1 < q^2 < 1 \text{ (GeV/c)}^2$.

IV. THE SLAC MUON BEAM

The design of the muon scattering experiments at SLAC depends strongly on the beam properties, so I will describe it briefly, although a detailed description of the beam has been published.¹⁵ The muons are photoproduced in a thick target by the bremsstrahlung quanta of the primary electron beam incident on it. Most of the muons are produced in the first few radiation lengths by high energy quanta, and so their source has the same size as the incident electron beam, i. e., a diameter of a few millimeters. This is in marked contrast to the effective source provided by the decay of a high energy pion beam, which is typically 10 cm in diameter and tens of meters long, and it is the reason for the qualitative differences in the properties of the resultant beam. The layout of the SLAC beam is shown in Fig. 6. The muons are produced in a 10 radiation length target of water-cooled copper. Immediately after the target is a 5.5 m beryllium filter to reduce the pion contamination from 30% at production to 3×10^{-6} pions per muon. The contamination was measured directly at the 3×10^{-4} level with a reduced filter, and the appropriate pion attenuation length in Be was also measured.¹⁵ The effect of multiple Coulomb scattering in the filter is to make the muons emerging from it appear to come from a source roughly 2.5 cm in diameter, located about one meter downstream from the production target. The rest of the beam is very conventional particle optics, with liberal use of field lenses to cope with the somewhat larger than usual phase space. The beam is brought to a first focus at a momentum-defining slit, S1. The second stage of the beam produces an almost dispersion-free image of the muon source at S2. The third stage refocuses the beam at the hydrogen target, well clear of slits and collimators. The beam aperture is defined in the first two quadrupoles, and the momentum at S1 by collimators of quite normal length. Subsequently, the envelope of the beam stays well clear of any scatterer.

In each leg of the beam there is steel sufficient to stop a 12 GeV muon should it stray outside the beam. It does not play any part in the shaping of the beam envelope. Figure 7a shows a horizontal beam profile at the final focus. The full width at half maximum is 2.9 cm for 12 GeV muons. Layout constraints on the optics lead to a magnification in the vertical plane of 4 between the source and the first focus. At that point the beam is redefined by a 1 meter steel collimator with a 10 cm aperture: it would otherwise be too big in the vertical plane. The effect of this very modest collimator can be seen in Fig. 7b. The solid curve is the measured vertical beam profile. The intensity drops by three orders of magnitude in a distance of less than 2 cm. The dashed curve is the horizontal beam profile scaled to the same magnification as the vertical profile. It represents what would be expected in the vertical plane were there no collimator. I think this demonstrates that it would be quite possible to think in the future of "pencil" muon beams. There is very little halo at larger distances from the beam. Veto counters with a 15 cm diameter aperture surrounding the beam see typically less than 1% of the flux. The muon flux at 10 GeV is 10^5 muons/sec in a $\pm 1.5\%$ momentum bite. Details of the beam performance are given in Table 1.

V. THE SLAC MUON SCATTERING EXPERIMENT

At SLAC, electron scattering is measured using spectrometers having small solid angles and very precise momentum resolution. However, the muon beam provides only $10^5 \mu/\text{sec}$. This is a factor of 2×10^9 less than the available electron flux, and the phase space of the muon beam is 5×10^6 larger. Therefore, we are a factor of 10^{16} worse off, and must do a different kind of experiment. The experiment which I will describe uses a large solid angle detector to measure simultaneously the elastic scattering and the inelastic scattering of positive muons at all angles

between 1.5° and 15° , and for all energy losses resulting in a final muon whose momentum is not less than $3 \text{ GeV}/c$. The first results from this experiment are in the course of publication.^{16, 17} It is the first experiment to study inelastic muon scattering on hydrogen.

The apparatus used in this experiment is shown in Fig. 8. The target was two meters of liquid hydrogen. Thin plate spark chambers placed on each side of a large aperture magnet were used to determine the angle and momentum of the scattered muon. These chambers were followed by eleven geometrical collision lengths of thick plate spark chamber and steel absorber, in order to make sure that it was a muon which had been observed. The small magnet shown just downstream of the hydrogen target was used to deflect knock-on electrons away from the upstream spark chambers. In fact μ -e scattering was the most severe background problem in the experiment. It limited the data-taking rate and was the reason for the decision to study only μ^+ scattering. Also shown in Fig. 8 is a large thin plate spark chamber placed below the target in order to observe the recoil proton from elastic scattering events. The additional kinematical constraint of the proton angle will be needed to separate cleanly the elastic scattering from the single pion production. The triggering arrangement is seen more clearly in Fig. 9. Several veto counters along the beam line upstream of the hydrogen target defined the incident beam. Trajectories of muons leaving the beam line in the vicinity of the hydrogen target were roughly defined by various combinations of the counters in three hodoscope planes, the third being placed in the muon detector just upstream of the fifth spark chamber, at a depth of 5.3 collision lengths. Any allowed combination not in coincidence with a veto could trigger the spark chambers. Without vetoes, the trigger rate was typically one per 1500 muons. With vetoes it was as small as one per 140,000 muons, about 30% being accidentals. The inner

trigger counters could be switched out of coincidence to increase the minimum scattering angle from 25 mrad to 35 mrad. I will refer to data taken with 10 GeV/c muons and a trigger sensitive down to 25 mrad as "low q^2 data." "High q^2 " will mean data taken with 12 GeV/c muons and a trigger sensitive down to 35 mrad.

The incident muon flux was monitored during data taking by five small counter telescopes placed upstream of the hydrogen target which sampled the spatial distribution of the beam and were designed to give a sum insensitive to small changes in beam position or shape. This monitor counted roughly three percent of the incident muon flux. Periodic normalization was made at low counting rates to two counter telescopes which covered the whole beam. There was very little variation of the normalization during the whole experiment. Tracking with trigger counter singles and doubles and with a toroid which measured the electron flux incident on the muon production target was good. Corrections for dead time counting losses in this procedure were around 2%, and contribute negligibly to the uncertainty in the normalization.

The largest electronic effect entering into the normalization was a roughly 15% off-time due to random veto counts. Considerable care was exercised to make sure that this effect was properly understood and measured. To this end, random veto pulses were introduced into parallel, redundant circuits in the monitor and in the trigger logic. Variations in the off-time measured in the different circuits were taken to represent the precision with which it was known. The uncertainty in the normalization from this source is estimated at less than 1%. Overall, it is estimated that the incident muon flux was known to $\pm 3\%$.

A total of 700,000 pictures were taken. They were scanned for muons appearing to come from the target. Two scans have been made for all the data, three scans for part of it. Any event found in scanning was measured, either by hand or by the

Hummingbird flying spot digitizer. Events which did not pass the reconstruction programs were all hand measured. A second re-measurement has been made for most of the data processed so far. A scanning, measuring and analysis efficiency correction of 2% has been made to the "low q^2 " data.^{16, 17}

Geometrical efficiency factors depending on the angle and momentum of the scattered muons were used to weight each event individually. They were generated by a Monte-Carlo calculation which took into account the measured beam distribution in position and angle, and the positions of all spark chamber and counter boundaries as determined from surveys and from scatter plots of reconstructed events. Statistical errors in these calculations are negligible. Systematic uncertainties in the geometry factors are estimated to be less than 2%, excepting for some events at very small angles where they can be as big as 10%. These events are all in the first q^2 bin of our data.

Special scans for pion events have been carried out, with the result that less than 0.2% of the data is estimated to be due to pion interactions, or to the detection of pions from muon scattering events in which the muon was not detected. Target empty runs were made. The subtraction for target empty events was 7% in the low q^2 data, and about 4% for the high q^2 data analyzed so far.

Figure 10 shows a momentum distribution for muons scattered through angles between 30 and 60 mrad. The width of the elastic peak (± 250 MeV) is consistent with measurement uncertainties folded with the momentum spread in the incident beam. The tail due to unresolved single pion production can be seen. Since the recoil chamber contains on average two or more δ -ray tracks, measurements of the proton recoil to separate the elastic scattering will not be started until a sample of pictures containing good muons originating in the target and satisfying the fiducial criteria has been generated. The position of the elastic peak for the

10 GeV data is consistent with what we would expect on the basis of the beam transport calculations; we take the average muon momentum at the center of the hydrogen target as the mean of the results from the transport calculations and the elastic scattering. It is $9.96 \pm .05$ GeV/c. This must be known to determine q^2 . However, the energy loss of the muon is determined using the elastic peak value.

The reconstructed tracks of the muons were projected back into the hydrogen target and the distance of the closest approach to the beam axis within the target length was computed. More than 99% of the events in the low q^2 data had distances of closest approach of ≤ 7 cm. This criterion was used to select events, together with a requirement that the muon pass through a fiducial region in the spark chambers.

Radiative corrections to the data were calculated, starting from the work of Tsai.¹⁸ The main contribution comes from the radiative tail of the elastic scattering (i.e., from muon bremsstrahlung). This contribution and that from the tail of the (3/2, 3/2) resonance were calculated exactly. The inelastic continuum corrections are harder to estimate. Approximations to the cross sections were made using published photoproduction data,¹⁹ and a rough knowledge of the behavior of the inelastic form factors. Fortunately, the inelastic form factors are not very rapidly varying functions of q^2 , and the muon radiative corrections are small, so that we do not introduce serious uncertainties into the results by this procedure. The continuum corrections are less than 4% for the data I will present here. They were calculated by the "exact" method, and also using a peaking approximation. Similar results were obtained in both cases for the value of the correction. It is difficult to see why the peaking approximation should be so good, as examination of the dependence of the exact radiative cross section on the integration variables showed that large contributions come from outside the peak.²⁰

VI. INTERPRETATION OF THE DATA: FORMULAE

Inelastic lepton scattering, like elastic scattering, is presumed to go via one-photon exchange. Although the experimental evidence for this assumption is not yet strong there is at present no reason, experimental or theoretical, to doubt it. It is well known that all we can learn about the interactions of virtual photons with nucleons from experiments which detect only the scattered lepton is contained in two functions of q^2 and energy loss. The one photon exchange diagram is shown in Fig. 11. One way of making the separation between kinematics and the physics of the process is to use the cross sections σ_T and σ_0 defined by Hand.²¹ These can be expressed in terms of the differential scattering cross section by the equations:

$$\frac{d^2\sigma}{dq^2 dK} = \Gamma_T (\sigma_T + \epsilon \sigma_0) \quad (2)$$

with

$$\Gamma_T = \frac{\alpha}{2\pi |q^2|} \frac{K^2}{p^2} \left(1 - \frac{2\mu^2}{|q^2|} + \frac{2EE' - \frac{|q^2|}{2}}{\nu^2 + |q^2|} \right) \quad (3)$$

and

$$\epsilon = \left(\frac{2EE' - \frac{|q^2|}{2}}{\nu^2 + |q^2|} \right) \left/ \left(1 - \frac{2\mu^2}{|q^2|} + \frac{2EE' - \frac{|q^2|}{2}}{\nu^2 + |q^2|} \right) \right. \quad (4)$$

q^2 is the square of the momentum transfer, E , p , E' , p' are the energies and momenta of the incident and scattered lepton, μ is the lepton mass, $\nu = E - E'$ is the laboratory energy of the virtual photon. $K = \nu - \frac{q^2}{2M}$, where M is the mass of the target. Real or virtual photons with the same value of K produce final hadronic states with the same invariant mass. Γ_T is the "flux" of transversely polarized virtual photons and ϵ is the ratio of the fluxes of transverse and scalar photons. The σ 's are thought of as absorption cross sections for virtual photons and in the $q^2 \rightarrow 0$ limit, $\sigma_0 \rightarrow 0$ and $\sigma_T \rightarrow \sigma_{\gamma p}$, the real photoabsorption cross section for photons

of energy K . Virtual photons are not directly observable and the distinction between flux and cross section is arbitrary, except in the $q^2 \rightarrow 0$ limit. Gilman²² defines a σ_{trans} and $-\sigma_{\text{long}}$ which are $\frac{K}{(q^2 + \nu^2)^{1/2}}$ times Hand's; $(q^2 + \nu^2)^{1/2}$ is the laboratory momentum of the virtual photon. For values of $\nu \gg q^2$, the difference between Gilman and Hand is unimportant. However, in the region covered by the SLAC μ -p and e-p inelastic scattering experiments, the difference can be quite marked and the experimentalist who would like to see an energy-independent inelastic form factor (i.e., $\sigma = \sigma_{\gamma p} \times F(q^2)$) has a choice of which σ to use. The arbitrariness of the definition of the "virtual photon cross sections" when $q^2 \neq 0$ should serve as a warning that intuitive ideas about the variations of real cross sections may not be readily transferable, although it is helpful to have some relationship with the more familiar world of real particles. A detailed theory of the interaction would be expected to remove these ambiguities. For completeness, I give here the expression of Drell and Walecka²³ for the scattering cross section in terms of the structure functions, W_1 and W_2 .²⁴

It is:

$$\frac{d^2\sigma}{dq^2 dK} = \frac{2\pi\alpha^2}{q^4 p^2} \left((|q^2| - 2\mu^2) W_1 + \left(2EE' \frac{|q^2|}{2} \right) W_2 \right) \quad (5)$$

The e-p scattering data has been analyzed²⁵ using this formula.

The quantity νW_2 used in the analysis of the electron scattering data is related to σ_T by the expression:

$$\nu W_2 = \frac{1}{4\pi^2 \alpha} \left[\frac{1 - \frac{q^2}{2M\nu}}{1 + \frac{q^2}{2\nu}} \right] q^2 (\sigma_T + \sigma_0) \quad (6)$$

For large, fixed ν , νW_2 must approach zero as $q^2 \rightarrow 0$, since $\sigma_0 \rightarrow 0$ and $\sigma_T \rightarrow \sigma_{\gamma p}$ in this limit. In the low q^2 region it therefore seems useful to work in

terms of the σ 's, since σ_T in particular is directly related to $\sigma_{\gamma p}$. This is what we have done with the muon data. The impressive universality of the νW_2 curve for electron scattering makes it seem the most appropriate form to use in analyzing the data at high q^2 . However, without in any way suggesting that this is not so, I think that it is useful to look at other ways of analyzing the data as well, in order to get other perspectives on a very rapidly developing field. All the formulae quoted include the effect of the lepton mass explicitly in the $-2\mu^2$ term and implicitly in q^2 . σ_T , σ_0 , σ_{trans} , $-\sigma_{\text{long}}$, W_1 and W_2 depend only on the photon-target interaction. In order to separate transverse from longitudinal, or W_1 from W_2 , it is necessary to make measurements at the same q^2 , ν , but with different ϵ . The latter varies rather slowly with the kinematics, and this means that a separation must be done with widely differing incident energies and good statistics. The present muon data are not sufficient to make the separation. Values of ϵ in the present experiment are generally close to unity, and the analysis has been made in terms of $\sigma_{\text{exp}} = (\sigma_T + \epsilon\sigma_S)$.

VII. RESULTS OF THE SLAC EXPERIMENT ON HYDROGEN

A. Low q^2 Data^{16, 17}

A plot of $(\sigma_T + \epsilon\sigma_S)$ values obtained from the analysis of 81,000 pictures is shown in Fig. 12. 1,474 events with $K \geq 0.6$ GeV are included. Results for $K < .6$ GeV, including the elastic scattering, have not yet been analyzed. These data result from 7.8×10^8 muons incident on the full hydrogen target. 6.4×10^8 muons were run through the empty target to yield 104 events in the same kinematic range. Radiative corrections were less than 6% for most of the data, and nowhere more than 16.5%. The continuum correction was always less than 4%. The data are clearly consistent with the $q^2 = 0$ points, which are taken from bubble chamber

results.¹⁹ The "virtual cross section," σ_{exp} , falls off much more slowly than $(1 + q^2/0.71)^{-4}$. These results also show quite definitely that a $(1 + q^2/m_\rho^2)^{-2}$ dependence is too strong: the χ^2 probability for such a strong q^2 dependence is 67 for 22 degrees of freedom when we use only the muon data, 148 for 27 degrees of freedom if we use also the data of Ref. 19. An analysis in terms of the Sakurai²⁶ vector dominance model, restricted to the data with $K \geq 2$ GeV, gives a best fit to the ξ parameter of $1.2 \pm .2$, and a confidence level for the fit of 50%. The Tsai²⁷ variant of the theory gives a slightly better fit. A simple $(1 + q^2/m_\rho^2)^{-1}$ dependence of $(\sigma_T + \epsilon\sigma_0)$ also gives a good fit. (It should be noted that a good fit to these predictions is only meaningful if σ_T/σ_0 is found to be proportional to $\frac{q^2}{m_\rho^2}$). If the data including the $q^2 = 0$ points are fitted to $\sigma_{\text{exp}} = S_K(1 + Rq^2)^{-1}$, the fitted S_K values are consistent with the photoproduction results, and R is found to be $1.38 \pm .22$ GeV/c⁻². The confidence level for this fit is 65% and it is the one shown in Fig. 12. Use of the Gilman σ_{trans} and $-\sigma_{\text{long}}$ in such a fit to an energy independent form factor gives a value for R of $(2.16 \pm .26)$ GeV/c⁻², and an 85% confidence level. The slightly better fit shows that some of the energy dependence has been taken out, but the statistics are quite clearly not sufficient to demonstrate which form would give the best agreement. We have also made fits of the form $\sigma_{\text{exp}} = S_K(1 + Aq^2)^{-2}$. If A is not constrained to be equal to $\frac{1}{m_\rho^2}$, we get a 50% confidence level for the fit and an A value of $.58 \pm .09$. This form and the inverse linear one with $R = 1.37$ differ by only a few percent in the region covered by the low q^2 data and we cannot, therefore, distinguish between them. The inverse quadratic fit would be inconsistent with the electron scattering data²⁵ if extended out beyond our q^2 range into the region where νW_2 is roughly constant. Despite the variety of forms used to fit the data, the values of $\sigma_{\gamma p}$ predicted when we use only the muon data do not fluctuate a great deal; it seems that we would be

able to predict $\sigma_{\gamma p}$ to within 20% even if we did not have any guidance on which fit to use. However, we already know the absorption cross section for real photons to much greater precision from other sources.²⁸

B. Muon-Electron Comparison

I said at the beginning of my talk that one of the main reasons for doing muon experiments is to see if the muon behaves always exactly like the electron. Inelastic scattering places less restrictions on the outcome of the interaction and therefore may be more revealing than elastic scattering. In addition, there are experimental reasons which make it easier in some respects to compare muons and electrons using inelastic data. The cross section is very much bigger at high q^2 , and varies more gently. The data in the SLAC muon scattering experiment will extend out beyond a q^2 of $3 (\text{GeV}/c)^2$. Even with moderate statistics, this large range of q^2 should give the experiment great sensitivity to a $(1 + q^2/\Lambda^2)^{-2}$ factor in the cross section, which one might expect a muon-electron structure difference to produce. Such a large range in q^2 reduces the effect of systematic normalization uncertainties. To balance this, there are the difficulties. The cross section depends on q^2 , K and ϵ . The muon and electron data are obtained in different ways: the muons are detected at all angles but fixed incident energy; the electrons at a few fixed angles and a few fixed incident energies. In order to use the limited quantity of muon data to best advantage, it will be necessary to interpolate between the electron data points using a function with not too many parameters which represents the data reasonably well. The smoothness and range of validity of the "universal" curves for the e-p data suggest that we are again fortunate: a few parameters should suffice to give a good fit. The problem which is likely to give rise to the greatest controversy is the adequacy of the radiative corrections. In the case of the electron data,²⁵ the corrections are large but there is a vast amount of data with which to

check the internal consistency of the procedures. The muon experiment has small corrections but also few data. Some iteration is needed to check that the continuum corrections are not sensitive to the assumptions made.

You will have gathered from this preamble, that we do not have a result for the comparison which we would consider final. However, the data from both experiments is now in print, and it would be better for me to show you how it stands at present than to leave everyone to his own devices. Much more muon data will be forthcoming in the next few months.

In order to make the comparison, values of σ_{exp} have been taken from the 7 GeV and 10 GeV, 6° e+p scattering data.²⁹ The 7 GeV data is, of course, not directly comparable with the muon data taken with 10 GeV muons, since $\sigma_{\text{exp}} = \sigma_T + \epsilon \sigma_0$, and ϵ is different in the two cases. However, the differences in ϵ are very small in the region of interest, (never more than 6%) so that the comparison should still be valid. To interpolate between the electron data points and the real photon total cross section results quoted in Ref. 19, it was assumed that σ_{exp} could be represented by

$$\sigma_{\text{exp}} = \frac{S_K}{1 + R_K |q^2|}$$

Such a function gives a good fit to the existing muon data, and has the behavior expected at high q^2 in the region of roughly constant νW_2 . The electron data used is shown in Fig. 13, together with the muon and photon data shown previously.

S_K and R_K were determined at each value of K . R_K varied between 1.25 and 2.5 $(\text{GeV}/c)^2$. The ratios of the muon to the interpolated electron cross sections were calculated. If we assume that there is no q^2 or K dependence of the μ/e ratio, we obtain a value of $1.04 \pm .03$ for the normalization, where the error is only statistical in the muon data. The χ^2 for $\mu/e = 1.0$ is 21 for 26 degrees of freedom.

The true uncertainty in the ratio should include $\pm 6\%$ normalization uncertainty for the muon data, an estimated $\pm 5\%$ for the electron and photon values, and some allowance for a possibly oversimplified fit. The combination of all uncertainties leads to a result $\mu/e = 1.04 \pm .09$. This is a ratio of cross sections. It is more than one, but less than two standard deviations from the comparable number of 0.92 obtained in the elastic μ -p, e-p comparison.¹² A plot of the ratios is shown in Fig. 14. There is a slight tendency for the ratio to rise as q^2 increases, however the data is consistent with $\Lambda = \infty$. We do not consider it to be particularly significant at present; it shows qualitatively that muon inelastic scattering is like photo-production at low q^2 and like inelastic-electron scattering at moderate q^2 and it demonstrates that there are no normalization problems.

C. High q^2 Data

The data are obtained from 4×10^9 positive muons with momentum 12 GeV incident on the full hydrogen target. There are about 7 times as much data still in the course of analysis. Empty target subtractions are 4%. The results are preliminary and are given here to demonstrate the general trend of the data and the scope of this experiment. Figure 15 shows plots of σ_{exp} in the range $0.5 \leq |q^2| \leq 3 \text{ GeV}/c^2$ and $1.0 \leq K \leq 7.0 \text{ GeV}/c$. The continuing slow decrease of σ_{exp} with $|q^2|$ can be seen. The small crosses are e-p data points. It is clear that the trend of the "low q^2 " μ/e ratios will not persist; if anything, the "high q^2 " muon data at $1(\text{GeV}/c)^2$ are lower than the electron data. It should be emphasized that the data is preliminary. When the analysis is complete, the data will extend to well beyond $q^2 = 3 \text{ GeV}/c^2$, and should be capable of competing seriously with the muon g-2 experiment for the honor of setting the highest limit on a QED violation parameter.

VIII. SCATTERING FROM COMPLEX NUCLEI

The one photon exchange formalism applies to nuclei just as well as to nucleons. There are still two, and only two, form factors. At large four-momentum transfers, we expect to see the scattering as the incoherent sum of the contributions from the individual nucleons. Fermi momentum effects should be small at large energy loss. There is, however, a subtle and quite surprising effect which complicates this picture. It is very well known that the vector mesons, the ρ in particular, can be photoproduced coherently on nuclei by real photons via a diffraction type of mechanism. This type of mechanism, illustrated in Fig. 16, can operate equally well with virtual photons and at surprisingly high q^2 . The reason is that the nuclear form factor effects do not depend on q^2 directly, but on the momentum transfer to the target nucleus, whose minimum value, t_{\min} , is given by

$$t_{\min} = \left[\frac{|q^2| + M^2}{2\nu} \right]^2 \quad (7)$$

where M is the mass of the particle produced. The value of t_{\min} can be held constant in inelastic scattering at the value for real photons of energy E_γ , by maintaining the relationship

$$\nu = E_\gamma \left[\frac{M^2 + |q^2|}{M^2} \right] \quad (8)$$

between the energy loss of the lepton, ν , and q^2 . The direct influence of q^2 variation in such a process will be determined by how the photon-meson interaction depends on q^2 and not by the nuclear form factor, providing that this relationship is maintained. One of the most surprising aspects of the way in which coherent production processes affect the total photoabsorption cross sections is that they introduce an effective shadowing: total photoabsorption cross sections on complex nuclei should be less than A -dependent. This has been discussed by many authors. 30

In particular, Brodsky and Pumplin³¹ have considered real and virtual photoabsorption. In the vector dominance model, the photon-vector meson coupling does not depend on q^2 , and the shadowing effect should be roughly constant at constant t_{\min} . For real photons, at least 50% of the shadowing effect is guaranteed by the existence of the observed coherent production, independently of vector dominance. I am not entirely sure how to estimate what would be expected to happen at large q^2 if ρ dominance did not hold. I think that the shadowing would increase, at constant t_{\min} , if the ratio of diffraction-like processes on nucleons to all photoabsorption were to increase with $|q^2|$ and vice versa. Of course, a departure from pure A-dependence could arise from a difference between the scattering from protons and neutrons at large q^2 . This has been suggested by Bjorken and Paschos.³²

The first measurement of the inelastic scattering of muons from carbon was made by Hoffman et al.³³ Their results were consistent with an A-dependent cross section for both real and virtual photons. Muon carbon scattering data have also been obtained at SLAC and the first results are reported to this conference.³⁴ The experimental layout is the same as that shown in Fig. 8, the carbon target being placed just upstream of the hydrogen target position. Radiative corrections were slightly larger than in the case of hydrogen, being as big as 25% in the highest K , lowest q^2 bin. The continuum corrections were again small. Values of σ_{\exp} from these data were divided by the fit to the muon-proton data shown in Fig. 12. An average value of the ratio in the range $0.05 < |q^2| < .4$ $(\text{GeV}/c)^2$ was computed for each energy, and these values are shown in Fig. 17. Also shown are the data of Hoffman et al.,³³ Caldwell et al.,³⁵ and Meyer et al.,³⁶ The SLAC data show evidence of shadowing at photon energies > 3 GeV. They are consistent with the results of Refs. 35 and 36 but are in disagreement with the result of Ref. 33. However, the result of Ref. 33 is strongly influenced by two points at small q^2 .

with large error flags. A smooth curve can be drawn through the photoproduction data and the data of Ref. 33, to give quite an acceptable χ^2 , so that it may be just a statistical fluctuation.

The statistics of the SLAC experiment are not yet good enough to determine the q^2 dependence of the shadowing. A considerable amount of additional data is presently being studied, and some data from copper will also be analyzed.

Some nuclear emulsion measurements of muon inelastic scattering have been made.^{37, 38} The technique is difficult and tedious, and scanning biases are hard to evaluate, particularly in experiments with very few events. A comparison of muon and electron inelastic scattering in emulsions³⁸ showed an apparent excess of muo-production. Most of the events in these experiments are at low q^2 and low K , and a correction has to be made to take into account the difference in the minimum q^2 possible in the two cases.

IX. COSMIC-RAY MUONS

Cosmic-ray experiments having a bearing on high energy muon interactions have been reviewed this summer by Wolfendale.³⁹ The outstanding anomaly in this field is the zenith angular distribution of high energy muons in the cosmic radiation.⁴⁰ The results of the Kolar Gold Field experiment⁴¹ are in disagreement with the results of Ref. 40 and are close to what would be expected if cosmic-ray muons are mainly produced by pion decay in the upper atmosphere. However, the data are not sufficient to disprove the Utah findings in a conclusive manner.

ACKNOWLEDGEMENTS

Much of my talk has been devoted to the results of the SLAC muon scattering experiment, which are due to the very hard work of my colleagues in the group of

Professor Martin L. Perl. I am deeply indebted to them for their assistance and collaboration, and to Professor Perl also for his encouragement. I would like to acknowledge useful discussions with many members of SLAC; in particular, with F. Gilman and S. J. Brodsky. I am grateful to Professors Lederman and Knop for bringing the new e-p elastic scattering data to my attention.

REFERENCES

1. S. J. Brodsky, invited paper, this conference.
2. J. Bailey, W. Bartl, G. Von Bochman, R. C. A. Brown, F. J. M. Farley, H. Jostlein, E. Picasso, R. W. Williams, Phys. Letters 28B, 287 (1968).
3. J. Aldins, S. J. Brodsky, A. J. Dufner, T. Kinoshita, Report No. SLAC-PUB-635, Stanford Linear Accelerator Center (1969).
4. F. J. M. Farley, invited paper at 1st meeting of the European Physical Society, Florence (1969).
5. J. Bailey and E. Picasso, to be published in Reports on Progress in Physics (1969).
6. J. J. Russell, R. C. Sah, M. J. Tannenbaum, W. E. Cleland, D. G. Stairs, Abstract No. 48, presented at this conference.
7. N. M. Rosenbluth, Phys. Rev. 79, 615 (1950).
8. K. J. Barnes, Nuovo Cimento 27, 228 (1963).
9. L. M. Lederman and M. J. Tannenbaum, Advances in Particle Physics, Cool and Marshak (eds.) (Interscience Publishers, New York, 1968); Vol. 1.
10. See for example G. Weber in Proc. Int. Symp. Electron and Photon Interactions at High Energies, Stanford Linear Accelerator Center, 1967. (Clearing House of Federal Scientific and Technical Information, Washington, D. C., 1968). Also Ref. 12.
11. R. W. Ellsworth, A. C. Melissinos, J. H. Tinlot, H. von Briesen, Jr., T. Yamanouchi, L. M. Lederman, M. J. Tannenbaum, R. L. Cool, A. Maschke, Phys. Rev. 165, 1449 (1968). A review of earlier work may be found in Ref. 9.
12. L. Camilleri, J. H. Christenson, M. Kramer, L. M. Lederman, Y. Nagashima, T. Yamanouchi, Phys. Rev. Letters 23, 149 (1969), and Phys. Rev. Letters 23, 153 (1969).

13. T. Janssens, R. Hofstadter, E. B. Hughes, M. R. Yearian, Phys. Rev. 142, 922 (1966).
14. Ch. Berger, V. Burkert, G. Knop, B. Langenbeck and K. Rith, Abstract No. 28 presented to this conference. See the invited paper of J. G. Rutherglen (this conference) for a review of the electron data.
15. J. Cox, F. Martin, M. L. Perl, T. H. Tan, W. T. Toner, T. F. Zipf, W. L. Lakin, Nucl. Instr. Methods 69, 77 (1969); see also A. Barna, J. Cox, F. Martin, M. L. Perl, T. H. Tan, W. T. Toner, T. F. Zipf, E. H. Bellamy, Phys. Rev. Letters 18, 360 (1967).
16. B. Dieterle, T. Braunstein, J. Cox, F. Martin, M. L. Perl, W. T. Toner, T. F. Zipf, W. L. Lakin, H. C. Bryant, Report No. SLAC-PUB-651 (1969).
17. M. L. Perl, T. Braunstein, J. Cox, B. Dieterle, F. Martin, W. T. Toner, T. F. Zipf, W. L. Lakin, H. C. Bryant, Report No. SLAC-PUB-652 (1969).
18. Y. S. Tsai, Phys. Rev. 122, 1898 (1961);
L. W. Mo and Y. S. Tsai, Rev. Mod. Phys. 41, 205 (1969).
19. J. Ballam, G. B. Chadwick, R. Gearhart, Z. G. T. Guiragossián, P. R. Klein, A. Levy, M. Menke, J. J. Murray, P. Seyboth, G. Wolf, C. K. Sinclair, H. H. Bingham, W. F. Fretter, K. C. Moffet, W. J. Podolsky, M. S. Rabin, A. H. Rosenfeld, R. Windmolder, Report No. SLAC-PUB-618 (1969);
J. Ballam, G. B. Chadwick, Z. G. T. Guiragossián, P. Klein, A. Levy, M. Menke, E. Pickup, T. H. Tan, P. Seyboth, G. Wolf, Phys. Rev. Letters 21, 1541 (1968);
H. G. Hilpert, H. Schnackers, H. Weber, A. Meyer, A. Pose, J. Schreiber, K. Böckmann, E. Paul, E. Propach, H. Butenschön, H. Meyer, S. Rieker, H. Baisch, B. Naroska, O. Braun, P. Steffen, J. Stiewe, H. Wenninger, H. Finger, P. Schlamp, P. Seyboth, Phys. Letters 27B, 474 (1968).

20. W. L. Lakin, private communication.
21. L. Hand, Phys. Rev. 129, 1834 (1963).
22. F. J. Gilman, Phys. Rev. 167, 1365 (1968).
23. S. D. Drell and J. D. Walecka, Ann. of Phys. 28, 18 (1964).
24. In the case of elastic scattering, W_1 and W_2 are related to the elastic form factors of the target. See Refs. 22 and 23.
25. E. D. Bloom, D. H. Coward, H. DeStaebler, J. Drees, G. Miller, L. W. Mo, R. E. Taylor, M. Briedenback, J. I. Friedman, G. C. Hartman, H. W. Kendal, Report No. SLAC-PUB-642, Stanford Linear Accelerator Center (1969).
26. J. J. Sakurai, Phys. Rev. Letters 22, 981 (1969).
27. Y. S. Tsai, Report No. SLAC-PUB-600, Stanford Linear Accelerator Center, (1969).
28. A. Silverman, invited paper Sec. VI, this conference. (See Refs. 19, 35, 36)
29. Results for $(\sigma_T + \epsilon \sigma_0)$ were kindly supplied by J. Drees. The values were taken at the center of the K bins used in the muon analysis excepting for $K = 0.6 - 1.0$ where an average value was computed. The muon data are average values of σ_{exp} in the bin.
30. J. S. Bell, Phys. Rev. Letters 18, 57 (1964); L. Stodolsky, Phys. Rev. Letters 18, 135 (1967).
31. S. J. Brodsky and J. Pumplin, Report No. SLAC-PUB-554, Stanford Linear Accelerator Center (1969).
32. J. D. Bjorken and E. Paschos, Report No. SLAC-PUB-572, Stanford Linear Accelerator Center (1969).
33. C. M. Hoffman, A. D. Liberman, E. Engels, D. C. Imrie, P. G. Innocenti, R. Wilson, C. Zajde, W. A. Blanpied, D. G. Stairs, D. Drickey, Phys. Rev. Letters 22, 659 (1969).

34. W. L. Lakin, T. Braunstein, J. Cox, B. D. Dieterle, F. Martin, W. T. Toner, M. L. Perl, T. F. Zipf, H. C. Bryant, paper presented at this conference.
35. D. O. Caldwell, V. B. Elings, W. P. Hesse, R. J. Morrison, F. V. Murphy, and D. E. Yount, Abstract No. 33, presented at this conference (1969).
36. H. Meyer, B. Naroska, J. Weber, M. Wong, V. Heynen, E. Mandelkow and D. Notz, Abstract No. 23, presented at this conference (1969).
37. P. L. Jain, P. J. McNulty, Phys. Rev. Letters 14, 611(1965); J. A. Kirk, D. M. Cottrell, J. J. Lord, R. J. Piserchio, Nuovo Cimento 40A, 523 (1965); T. Konoshi, O. Kusomoto, S. Ozaki, M. Teranaka, T. Wada, Y. Watase, M. Ohta, Nuovo Cimento 54A, 781 (1968);
38. R. L. Thomson, J. J. Lord, J. A. Kirk, M. E. Nelson, R. J. Piserchio, Phys. Rev. 177, 2022 (1969).
39. A. W. Wolfendale, Rapporteur talk XI Int. Conf. on Cosmic Rays, Budapest (1969) (to be published in Acta Physica Hungarica).
40. H. E. Bergeson, J. W. Keuffel, M. O. Larson, E. R. Martin, G. W. Mason, Phys. Rev. Letters 19, 1487 (1967); H. E. Bergeson, J. W. Keuffel, M. O. Larson, G. W. Mason, J. L. Osborne, Phys. Rev. Letters 21, 1089 (1968). This is a re-analysis of the data contained in the previous paper; J. W. Keuffel, J. L. Osborne, G. L. Bolingbroke, G. W. Mason, M. O. Larson, G. H. Lowe, J. H. Parker, R. O. Stenerson, H. E. Bergeson, paper submitted to the XI Int. Conf. on Cosmic Rays, Budapest (1969) (to be published in Acta Physica Hungarica).
41. M. R. Krishnaswamy, M. G. K. Menon, V. S. Narasimham, S. Kawakami, S. Miyake, A. Mizohata, paper submitted to the XI Int. Conf. on Cosmic Rays, Budapest (1969) (to be published in Acta Physica Hungarica).

TABLE I

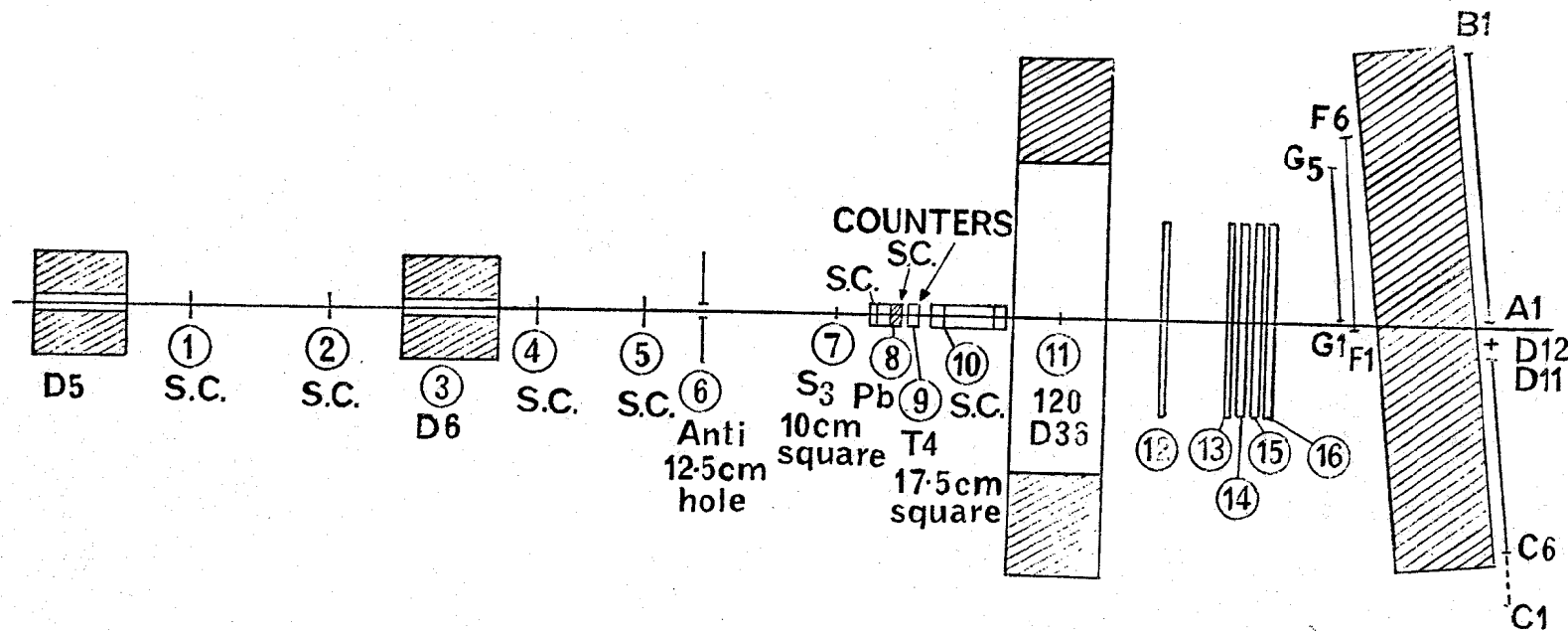
Beam Performance

Momentum	12.0	10.0	6.0	3.0	GeV/c
Momentum Bite	$\pm 1.5\%$	$\pm 1.5\%$	$\pm 1.5\%$	$\sim \pm 1.5\%$	
Flux for 100 KWatts of 16 GeV electrons	0.31×10^5	0.8×10^5	0.82×10^5	0.29×10^5	μ per second
Flux for 100 KWatts of 17 GeV electrons	0.59×10^5	1.03×10^5	-	-	"
Vertical beam width at S2 Full width at 10% intensity	9.5	9.8	9.8	10.6	cms
Horizontal beam width at S2 Full width at 50% intensity	2.9	3.2	5.4	4.8	"
Full width at 10% intensity	5.3	5.9	8.8	10.9	"
Vertical beam width at F3 Full width at 10% intensity	9.8	10.0	-	-	"
Horizontal beam width at F3 Full width at 50% intensity	2.4	3.0	-	-	"
Full width at 10% intensity	4.4	5.1	-	-	"

FIGURE CAPTIONS

1. Experimental arrangement in the muon trident experiment of Ref. 6.
2. Invariant mass distributions of muon pairs. (a) like muons, (b) and (c) unlike combinations.
3. Experimental arrangement in the muon-proton elastic scattering experiment of Ref. 12.
4. A typical example of a Rosenbluth straight-line plot.
5. Muon and electron results for the proton form factor. Representative points are shown from the experiments of Refs. 12 and 13.
6. Layout of the SLAC muon beam.
7. (a) Horizontal beam profile. (b) Vertical beam profile (solid curve).
8. Apparatus used in the SLAC muon scattering experiment.
9. Trigger counter arrangement in the SLAC muon scattering experiment.
10. Momentum distribution of scattered muons.
11. One photon exchange diagram for inelastic scattering.
12. Values of $(\sigma_T + \epsilon\sigma_0)$ obtained in the SLAC muon scattering experiment. The points at $q^2 = 0$ are obtained from the data of Ref. 19. The curve is a fit to the data described in the text.
13. Muon data and photon data for $(\sigma_T + \epsilon\sigma_0)$ as in Fig. 12. The additional points are electron scattering data from Ref. 25.
14. Values for the ratio of the muon scattering data shown in Fig. 13 to a fit to the photon and electron data shown in Fig. 13, described in the text.
15. Preliminary results for $(\sigma_T + \epsilon\sigma_0)$ obtained from muon-proton scattering at high q^2 .
16. Kinematics of diffractive muo-production.

17. Ratios of carbon to hydrogen photoabsorption cross sections obtained in muon scattering experiments and with real photons. The curves are the theoretical predictions of Brodsky and Pumplin.



D5, D6, 120D36 : BENDING MAGNETS

S.C. : SPARK CHAMBER

1502A1

Fig. 1

Experimental arrangement in the muon trident experiment of Ref. 6.

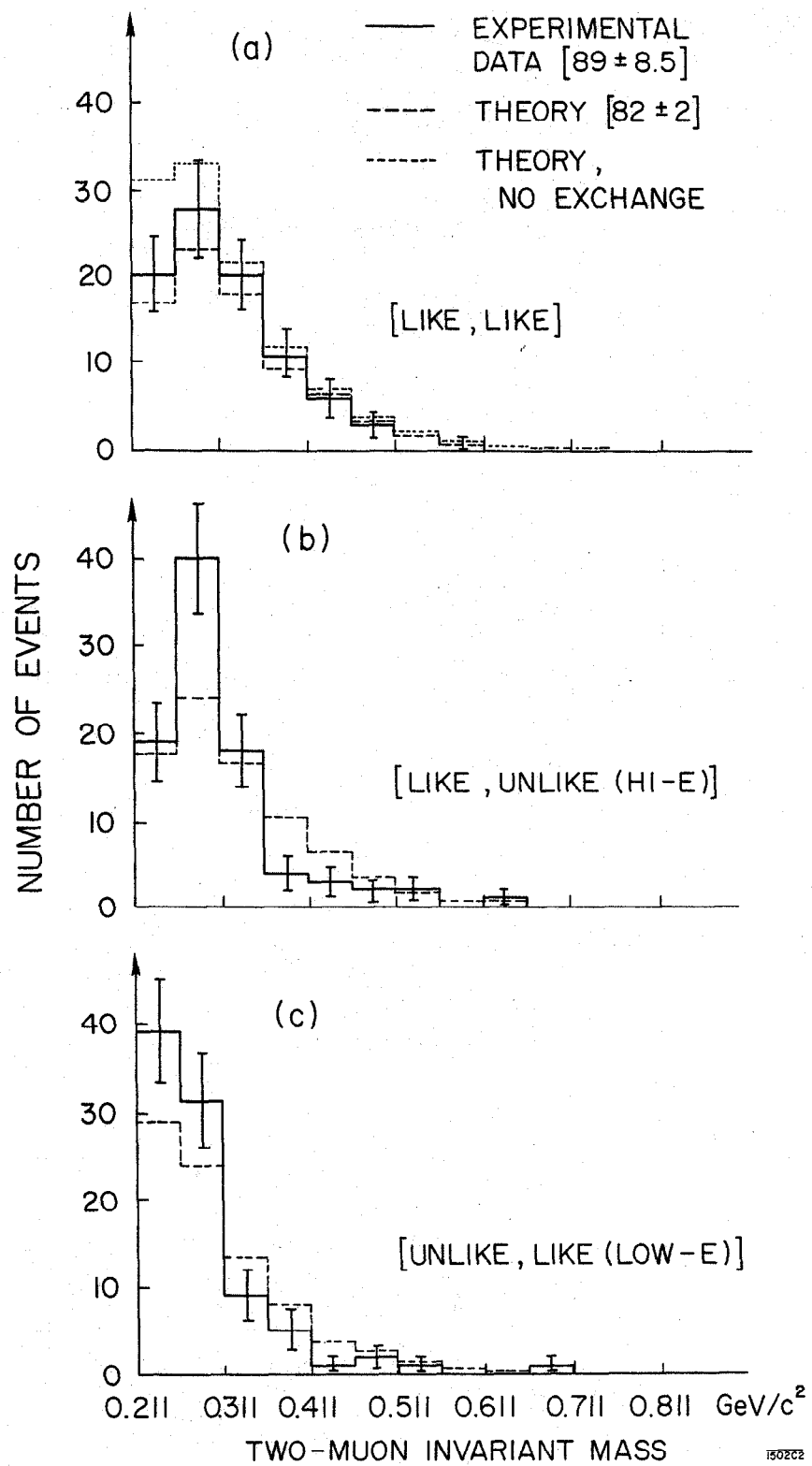


Fig. 2

Invariant mass distributions of muon pairs. (a) like muons, (b) and (c) unlike combinations.

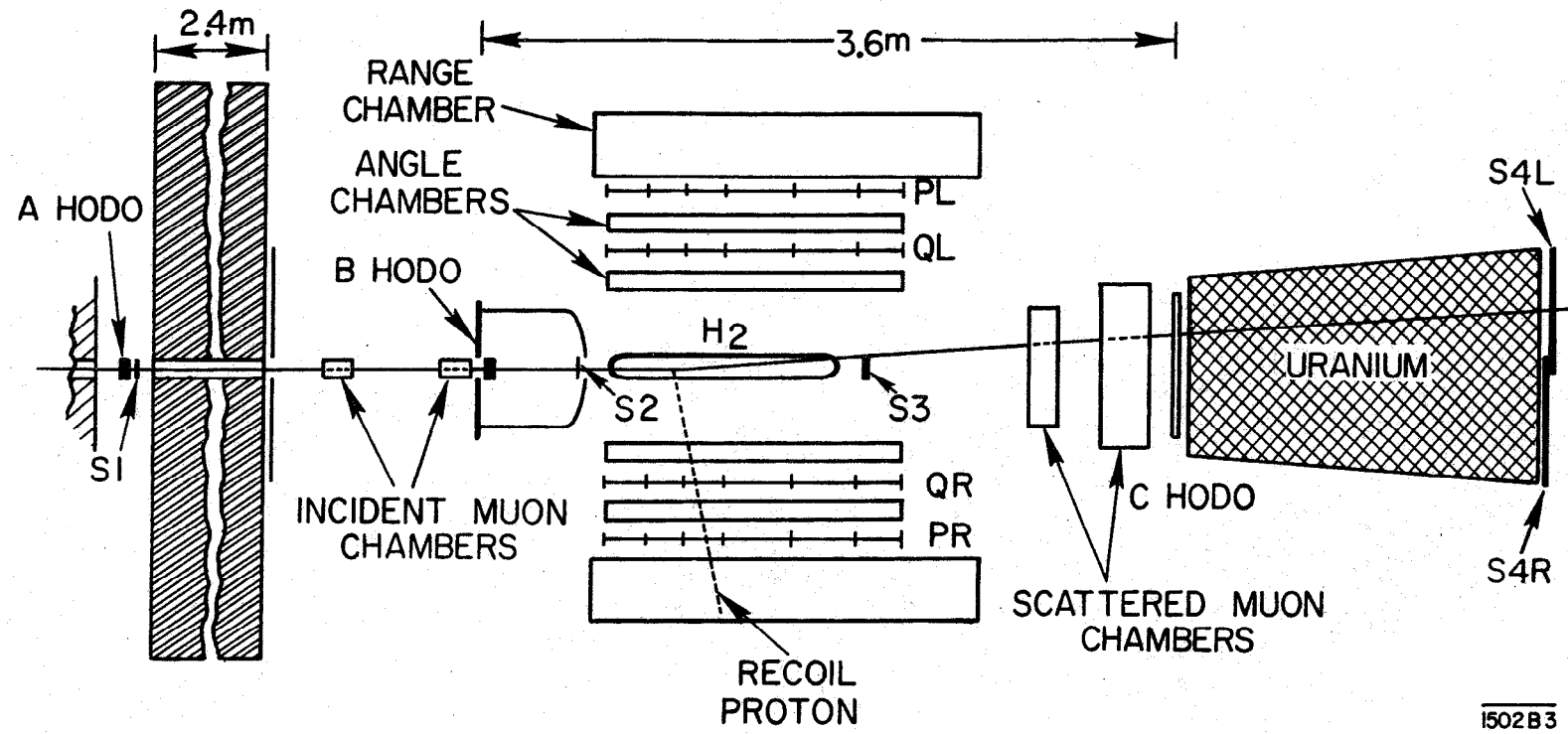


Fig. 3

Experimental arrangement in the muon-proton elastic scattering experiment
of Ref. 12.

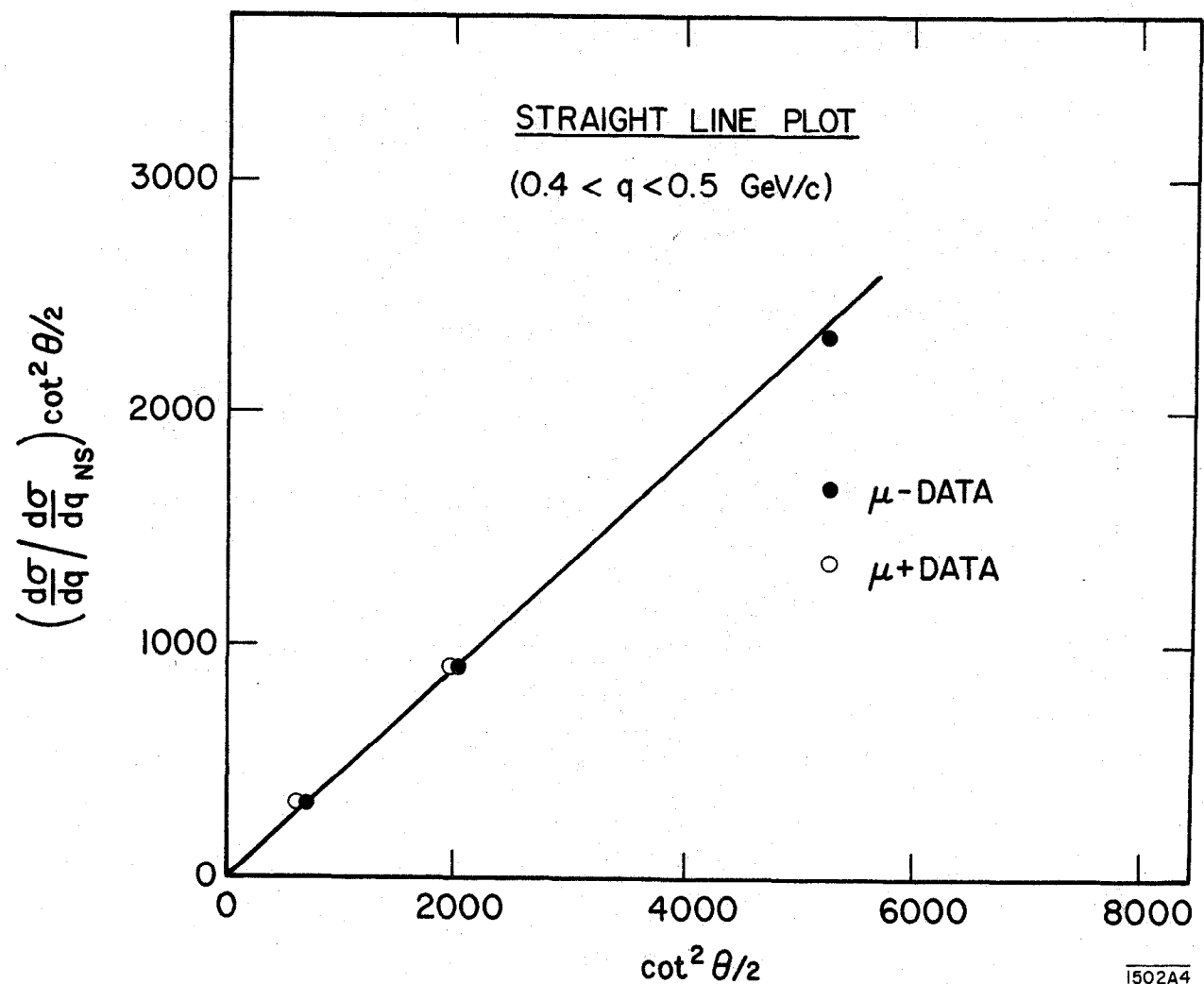


Fig. 4

A typical example of a Rosenbluth straight-line plot.

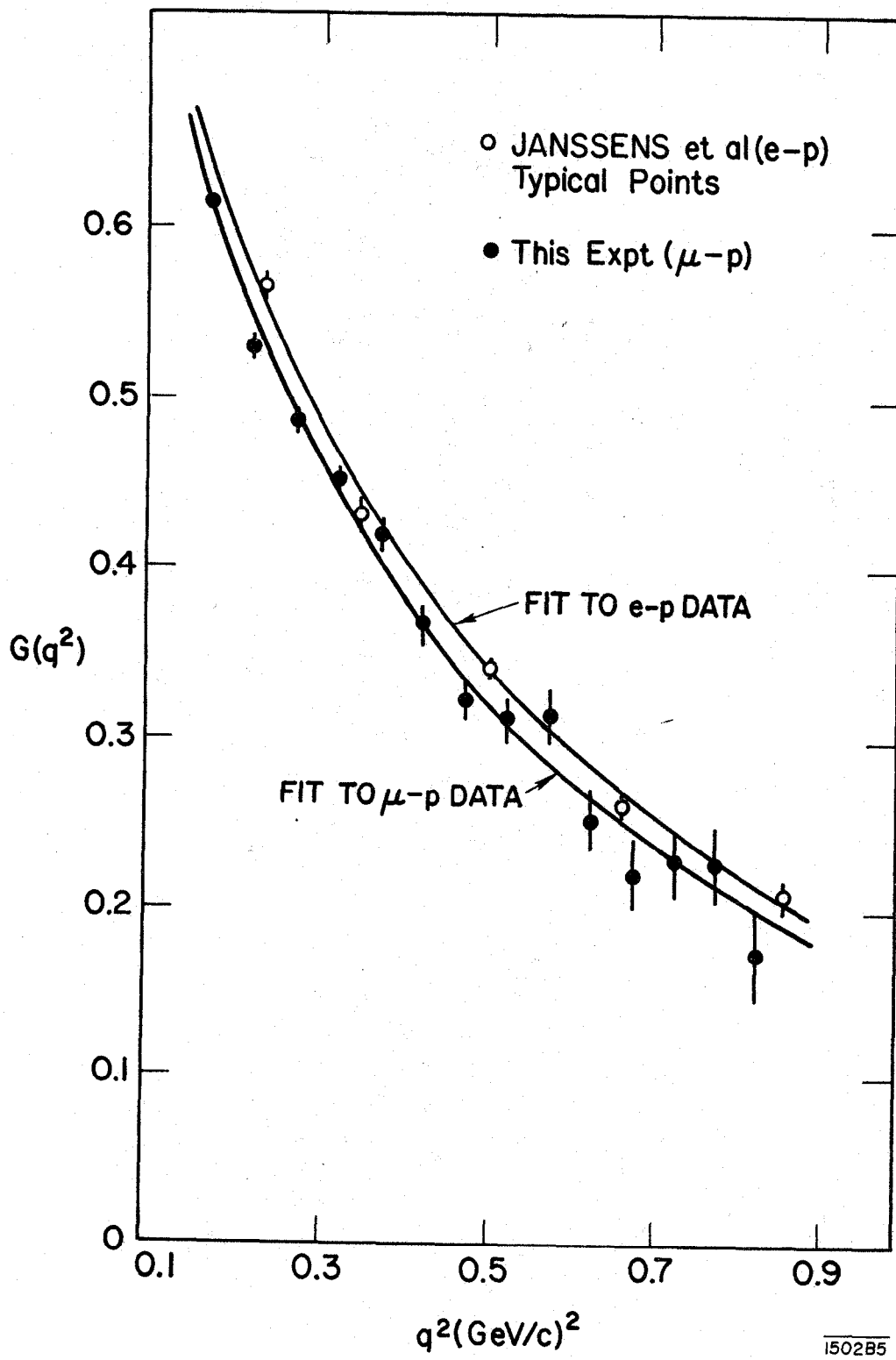


Fig. 5

Muon and electron results for the proton form factor. Representative points are shown from the experiments of Refs. 12 and 13.

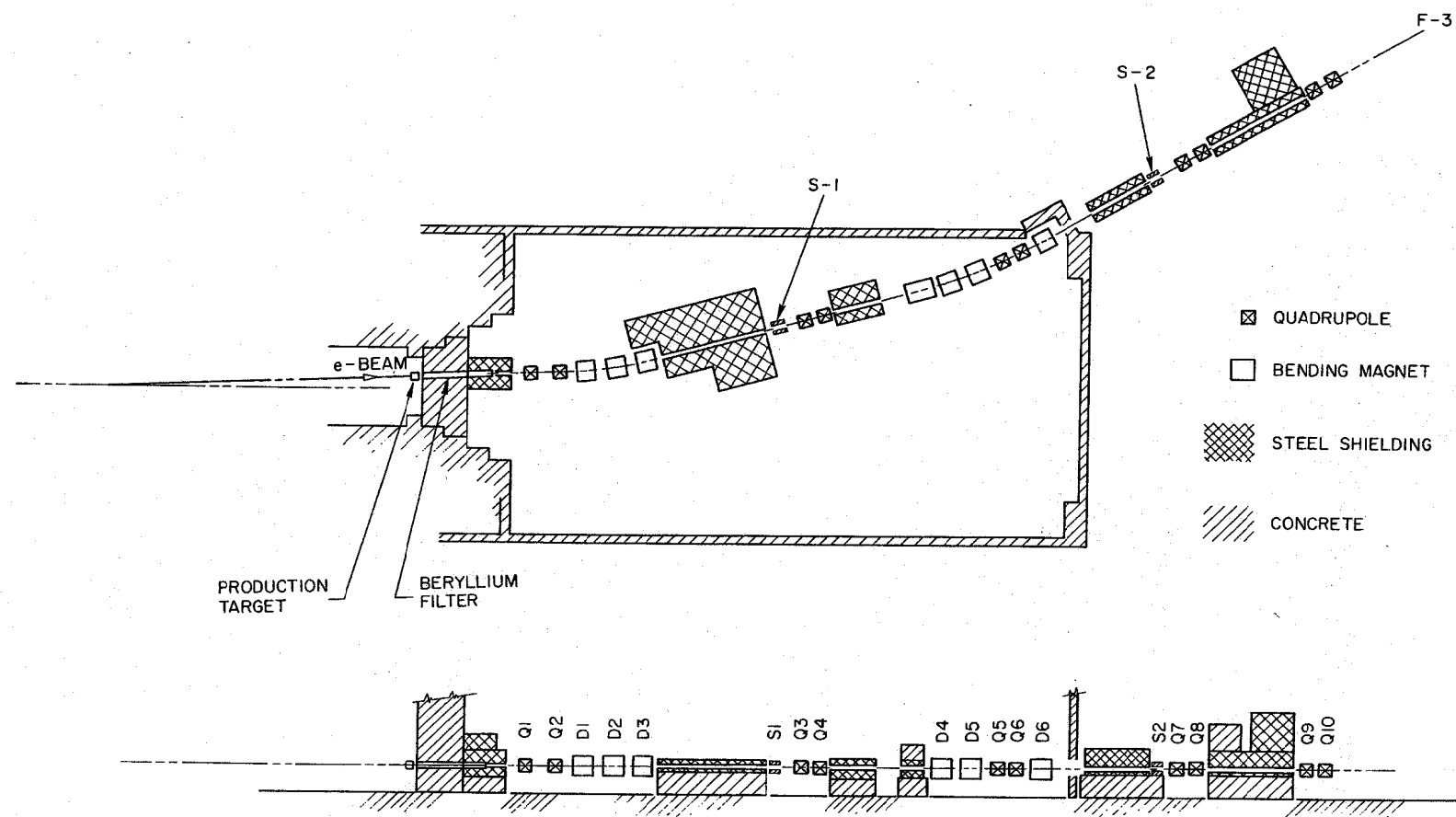
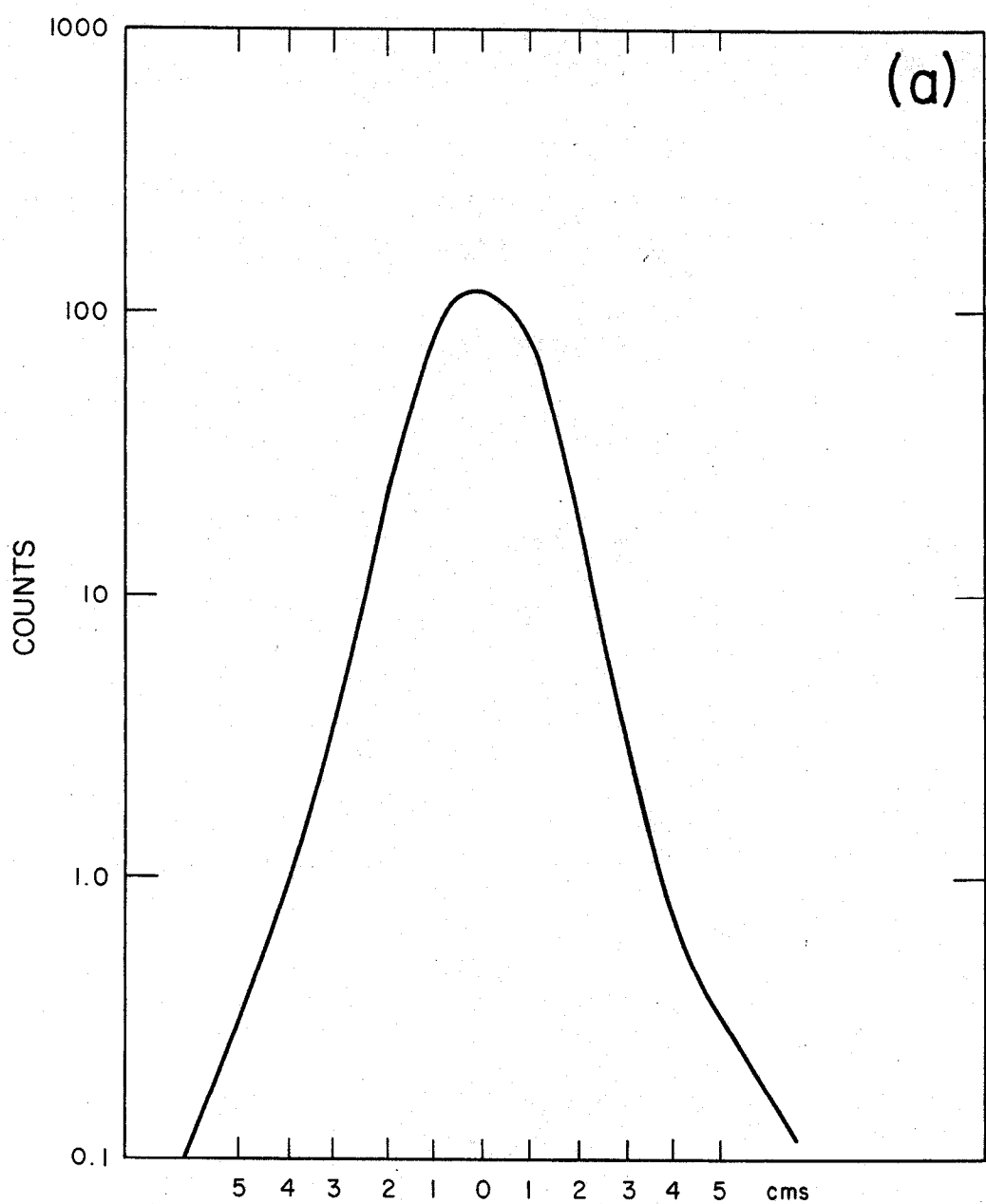


Fig. 6

Layout of the SLAC muon beam.

104368



1049BII

Fig. 7a

(a) Horizontal beam profile.

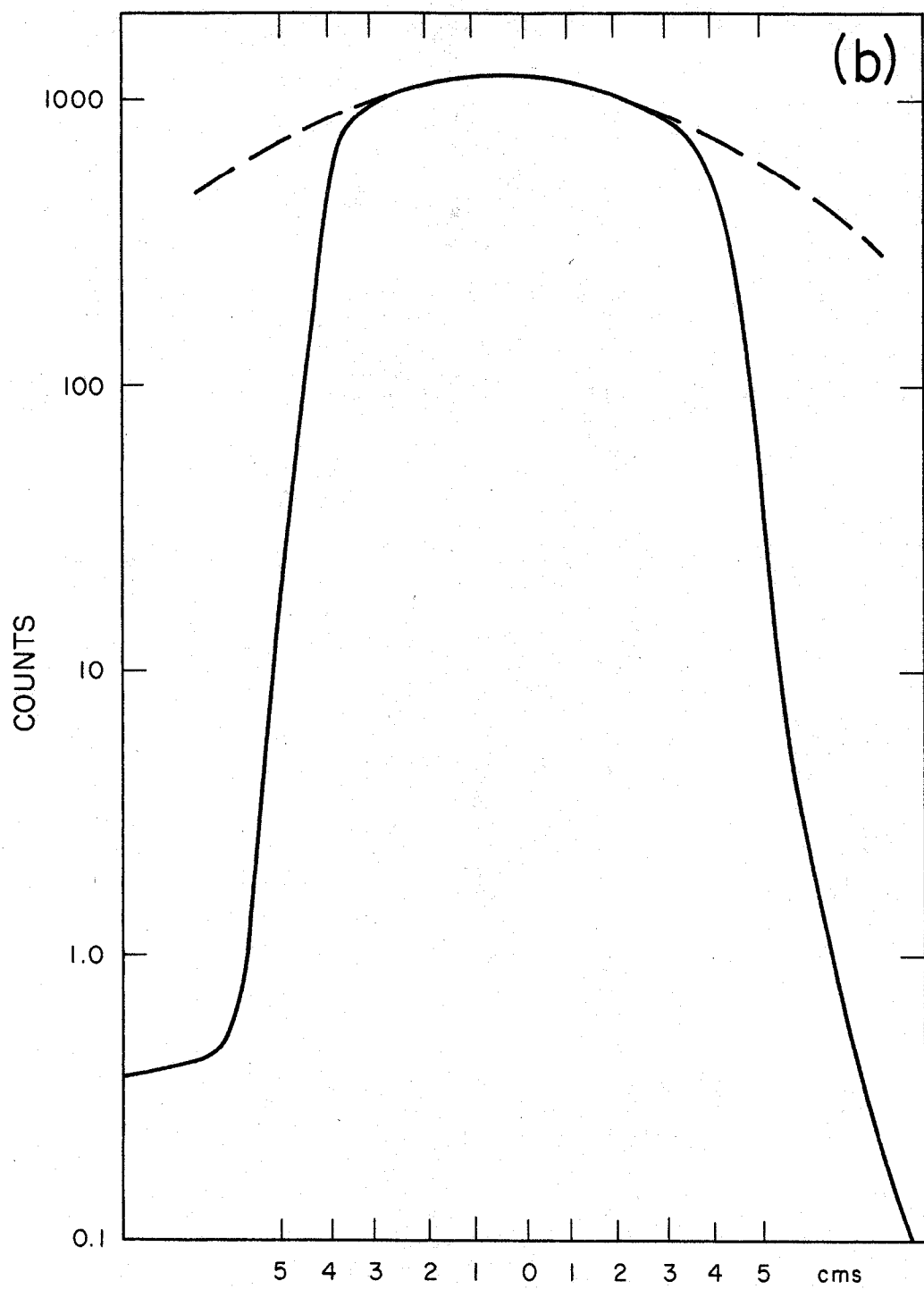


Fig. 7b

1049B12

(b) Vertical beam profile (solid curve).

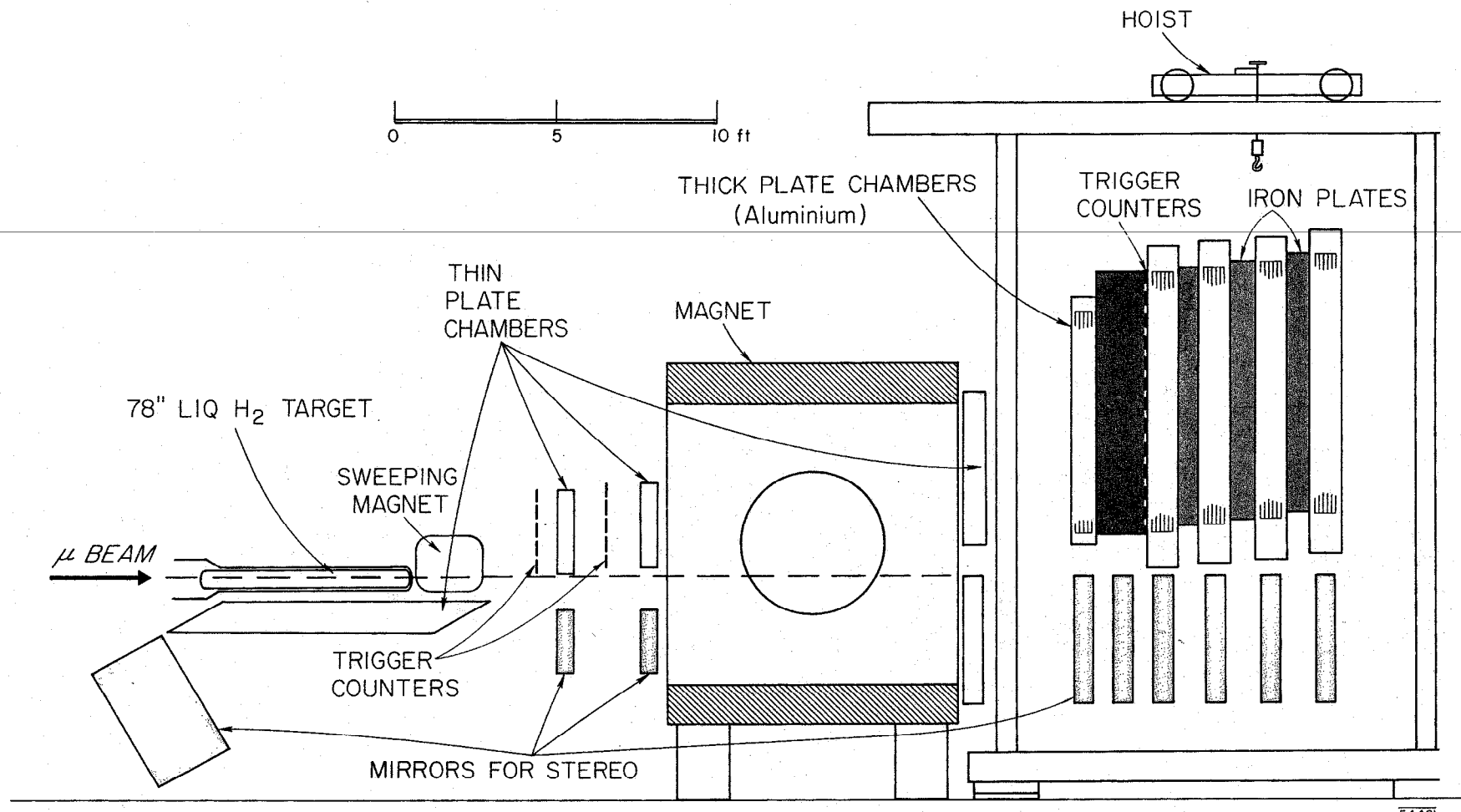
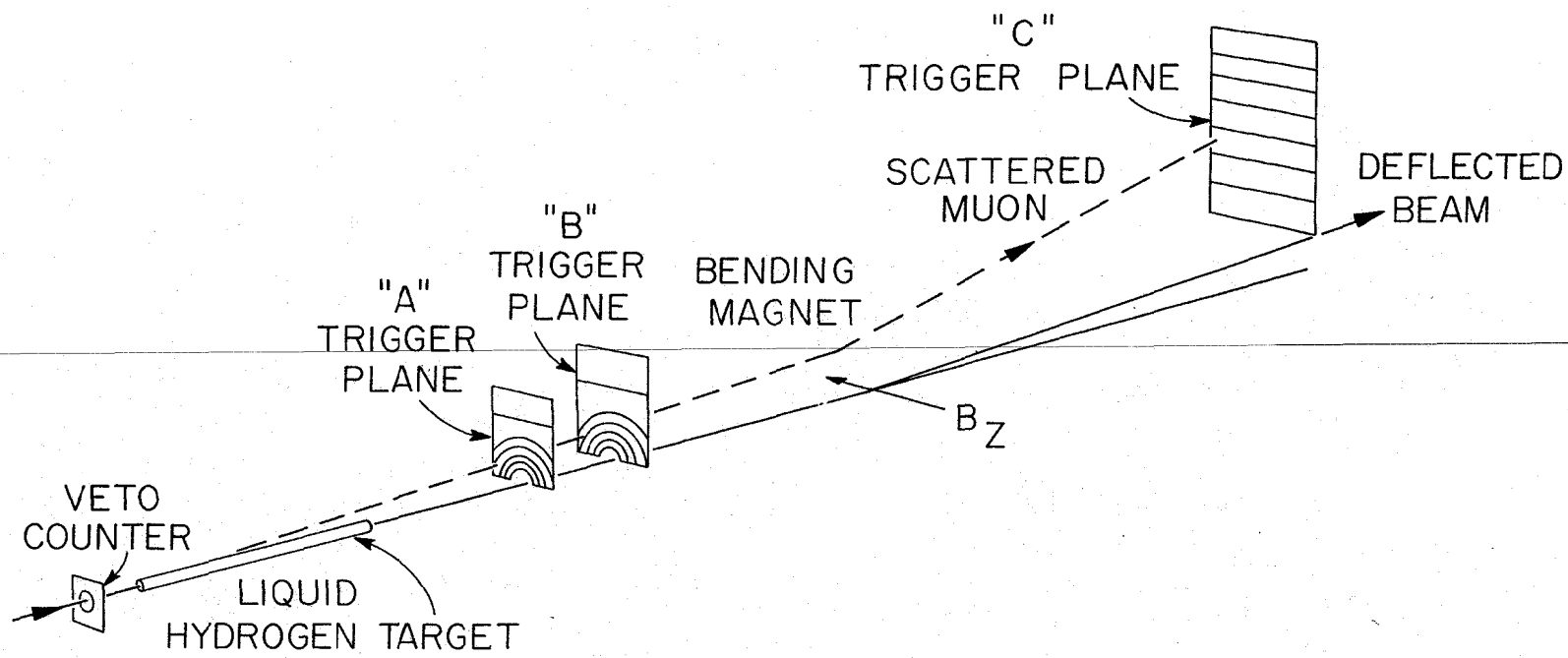


Fig. 8

Apparatus used in the SLAC muon scattering experiment.

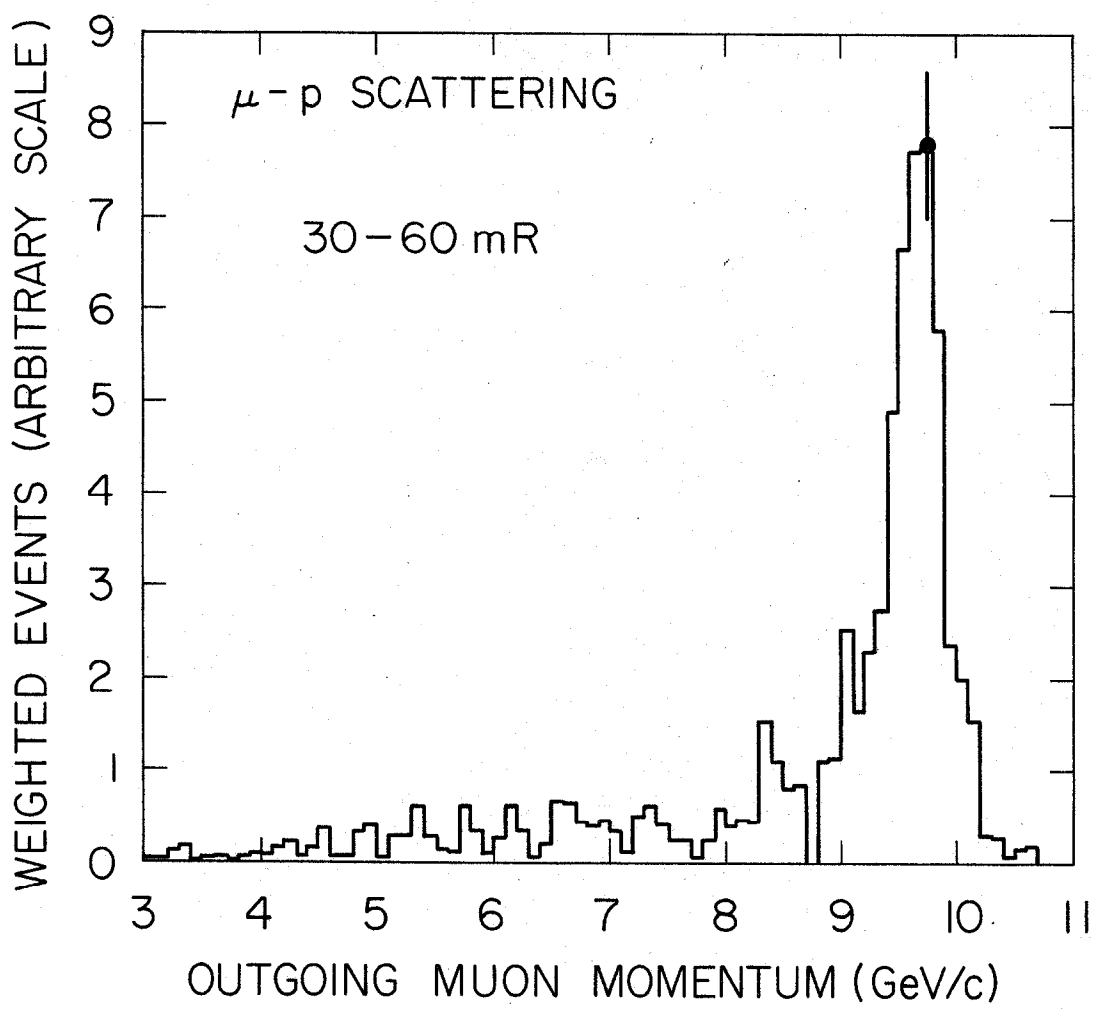


SCHEMATIC DIAGRAM OF MUON SCATTERING EXPERIMENT TRIGGER SYSTEM

1165C4

Fig. 9

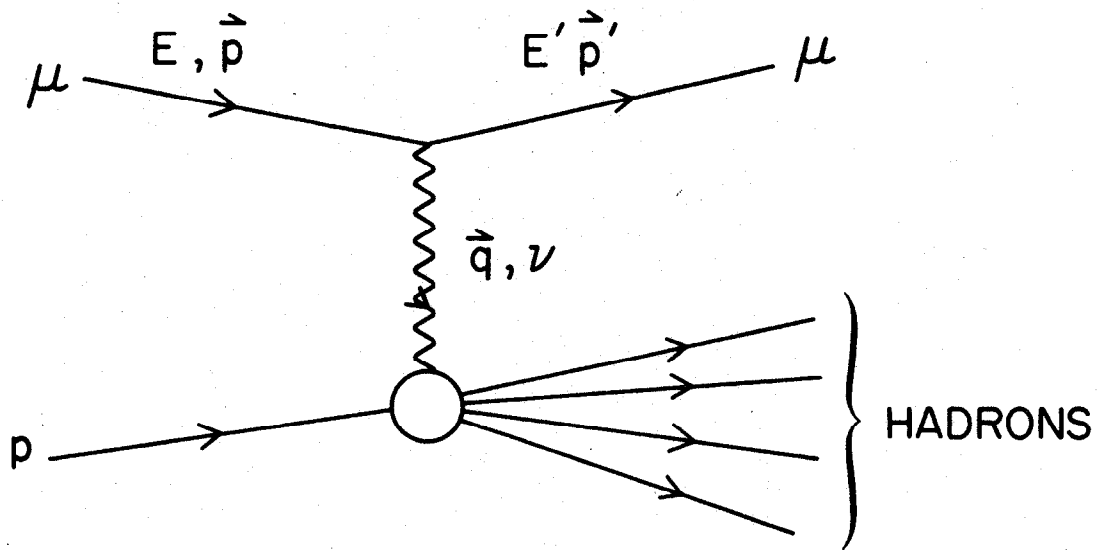
Trigger counter arrangement in the SLAC muon scattering experiment.



1433B1

Fig. 10

Momentum distribution of scattered muons.



1412A1

Fig. 11

One photon exchange diagram for inelastic scattering.

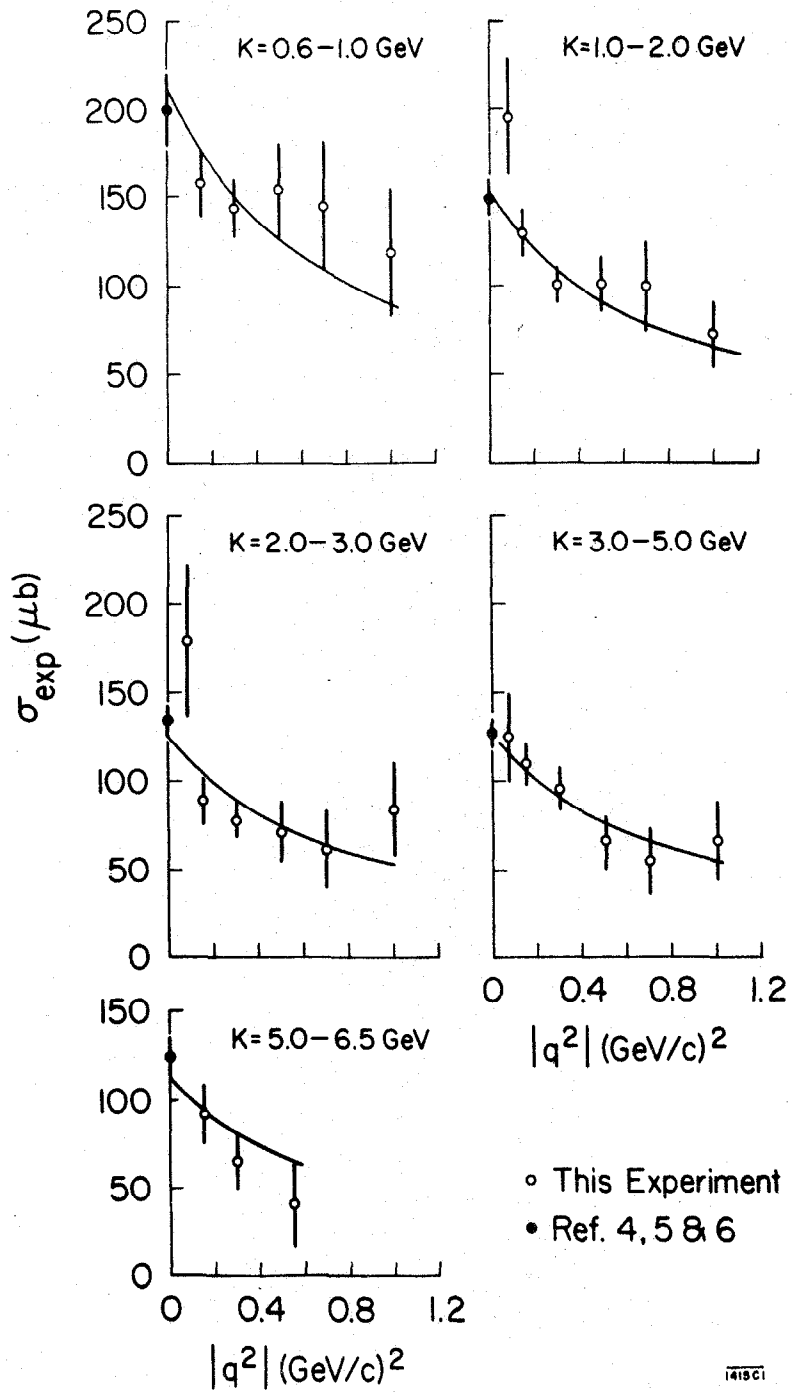


Fig. 12

Values of $(\sigma_T + \epsilon\sigma_0)$ obtained in the SLAC muon scattering experiment. The points at $q^2 = 0$ are obtained from the data of Ref. 19. The curve is a fit to the data described in the text.

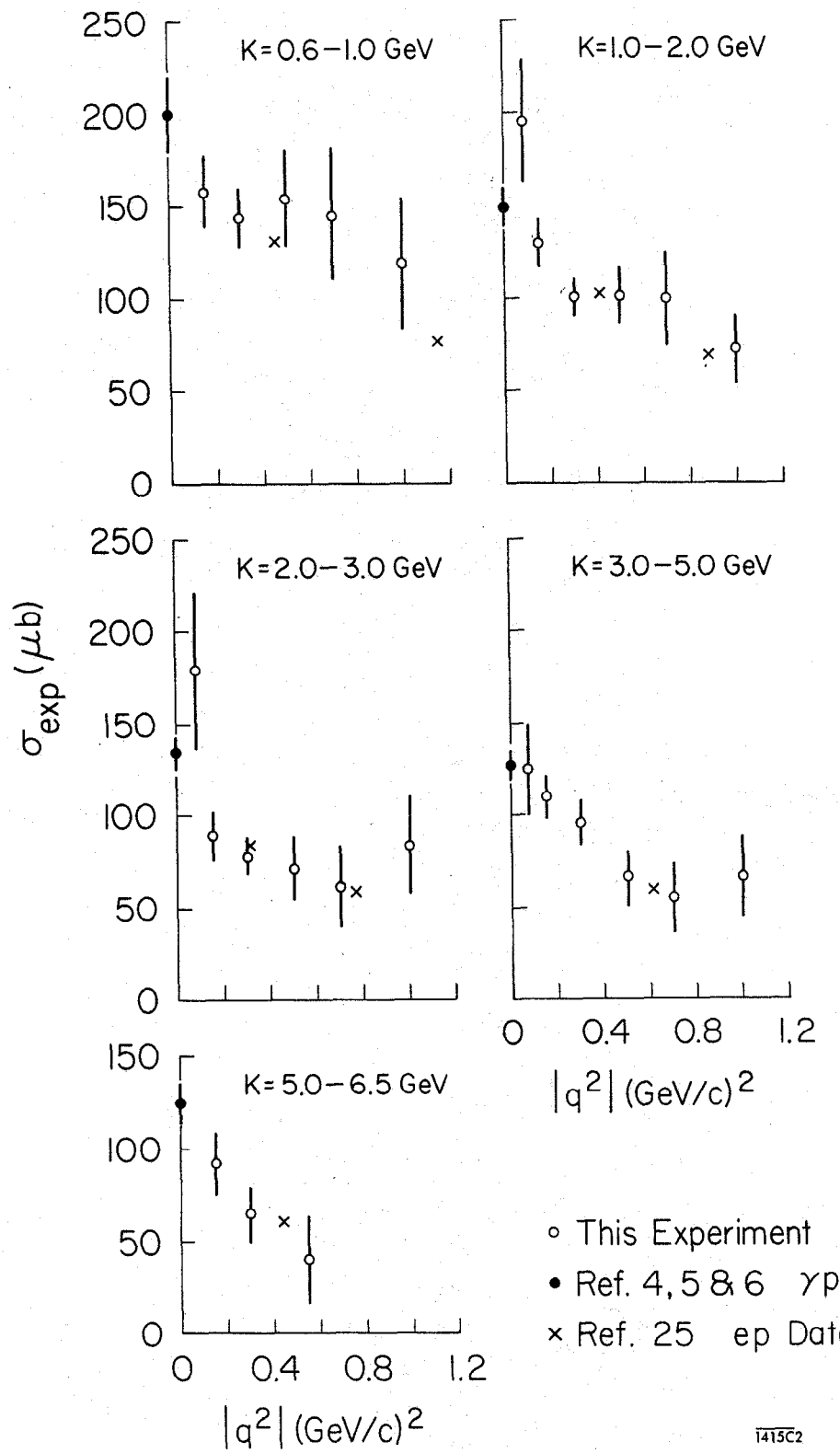


Fig. 13

Muon data and photon data for $(\sigma_T + \epsilon\sigma_0)$ as in Fig. 12. The additional points are electron scattering data from Ref. 25.

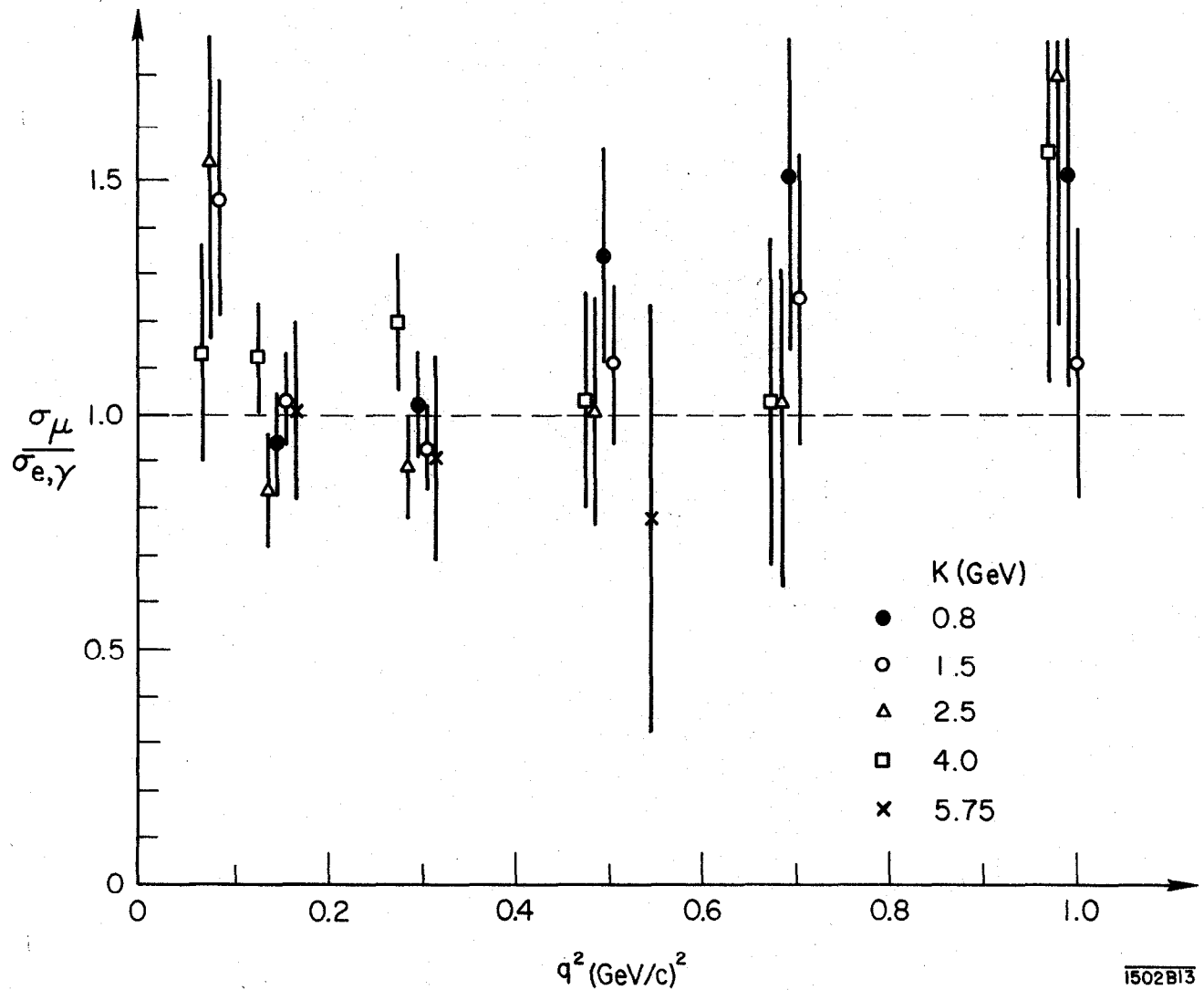


Fig. 14

Values for the ratio of the muon scattering data shown in Fig. 13 to a fit to the photon and electron data shown in Fig. 13, described in the text.

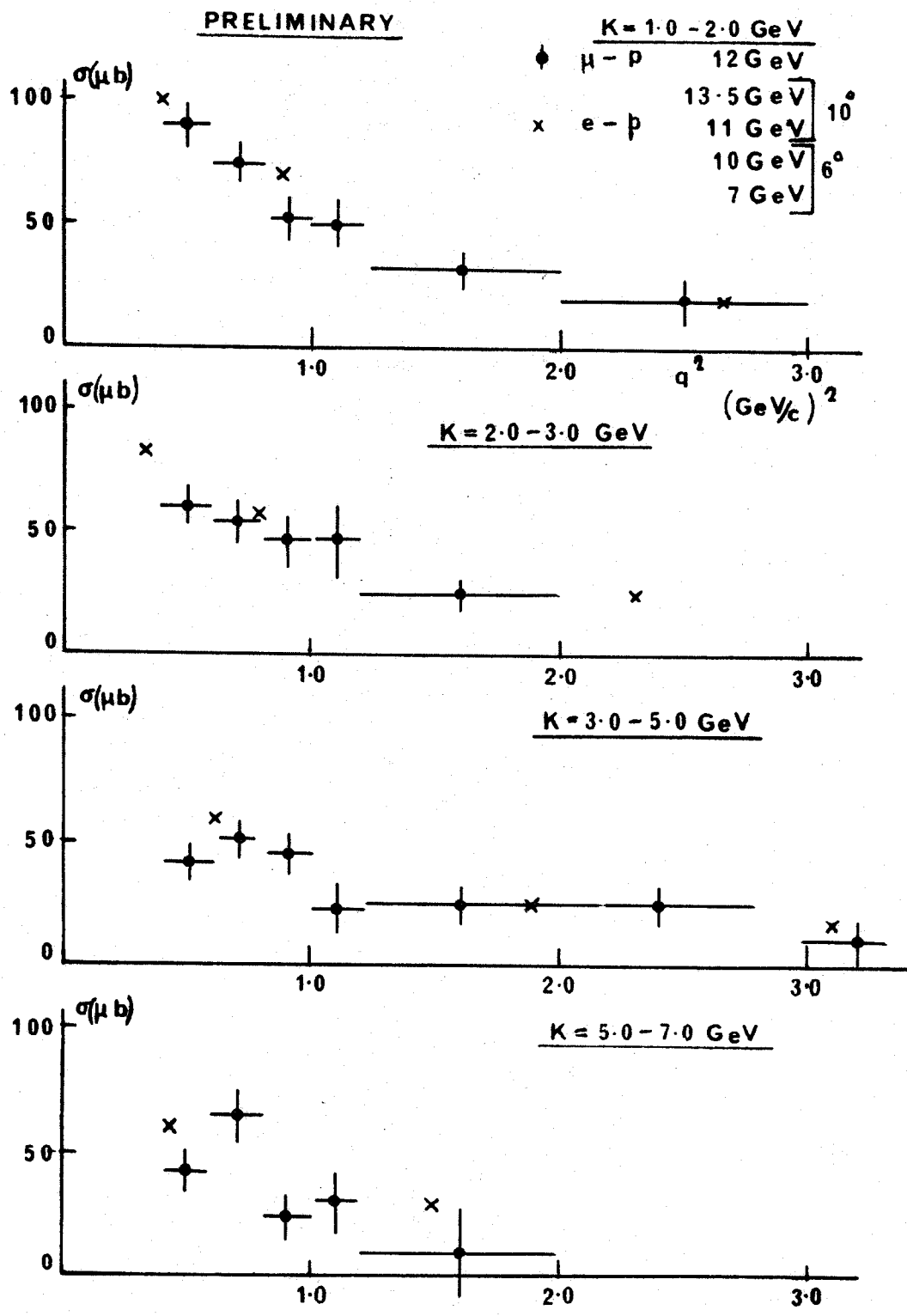
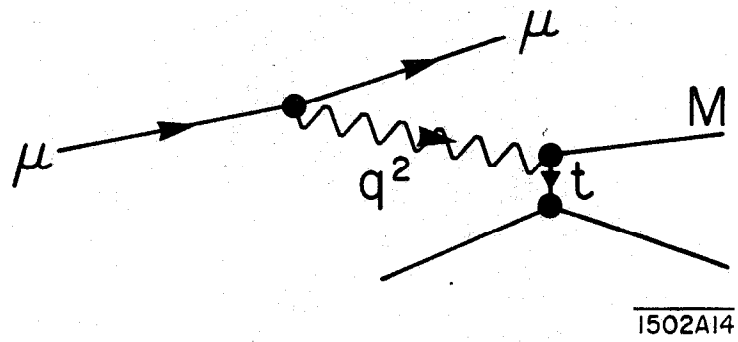


Fig. 15

Preliminary results for $(\sigma_T + \epsilon\sigma_0)$ obtained from muon-proton scattering at high q^2 .

1502A16



1502A14

Fig. 16

Kinematics of diffractive muo-production.

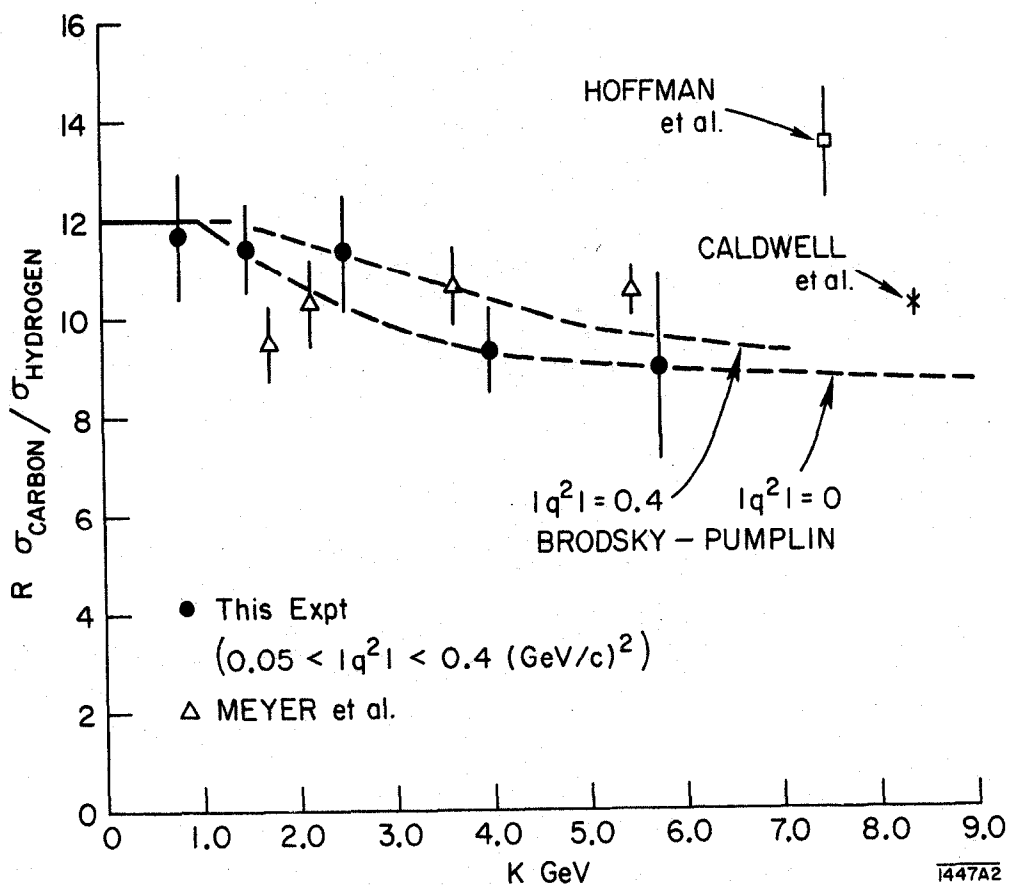


Fig. 17

Ratios of carbon to hydrogen photoabsorption cross sections obtained in muon scattering experiments and with real photons. The curves are the theoretical predictions of Brodsky and Pumplin.